

Characterizing Molecular Diffusion in the Lens Capsule

Problem Presenters

Melinda K. Duncan

Brian P. Danysh

Kirk J. Czymmek

Tapan P. Patel

University of Delaware

Problem Participants

Adam Anthony, Wichita State University

Chris Breward, Oxford University

David A. Edwards, University of Delaware

Michael Gratton, Duke University

Mansoor Haider, North Carolina State University

Yogesh Joshi, New Jersey Institute of Technology

Timur Milgrom, Clemson University

John A. Pelesko, University of Delaware

Gilberto Schleiniger, University of Delaware

Zunlei Xiao, University of Delaware

Twenty-Third Annual Workshop on Mathematical Problems in Industry

June 11–15, 2007

University of Delaware

Section 1: Experimental Setup

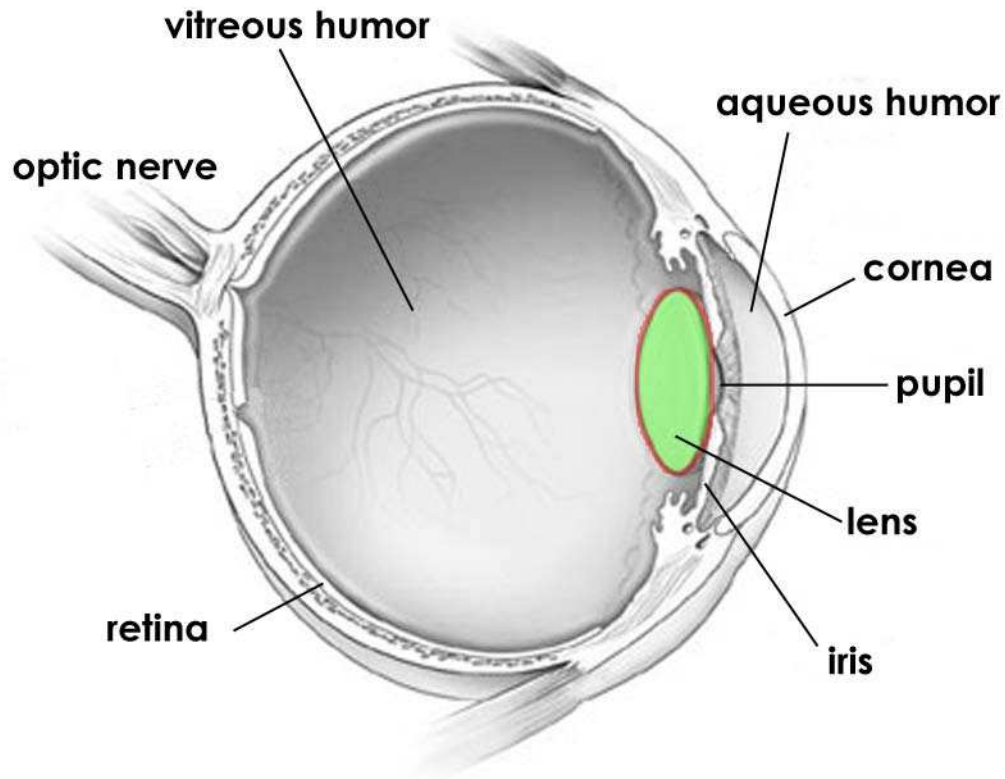


Figure 1.1. Picture of lens.

The lens is a transparent component of the eye which focuses light rays entering the eye to appropriate places at the back of the eye. It is tethered by muscles to the surrounding tissue and it is the movement of these muscles that alters the shape of the lens and allows focusing at different distances. The lens is sandwiched between two aqueous compartments: the aqueous humor in front of the lens and the vitreous humor behind (see Figure 1.1). The lens is an avascular tissue and relies on diffusion of nutrients and waste products for survival. It consists of highly specialized transparent cells surrounded by an outer membrane capsule. The outer membrane is a porous scaffold to which the cells underneath the membrane attach. The capsule allows force transmission and is selectively permeable. It is a complete seal around the lens and has thickness of $26\ \mu\text{m}$ in a human and $10\ \mu\text{m}$ in a mouse. There are various pore sizes (99% are 4–5 nm and 1% are about 10 nm) and these are small enough to prevent cells and some molecules from entering the layer. The scaffold is made from Collagen 4 and has sugar molecules bound on which extend into the pores and “wave in the wind”.

We are interested in studying diffusion through the lens capsule because diffusion is important for lens development and growth, nutrient and waste release, drug delivery, ocular inflammation and for cataract formation and treatment. To determine the diffusivity of various molecules through the lens capsule, experiments have been carried out using a technique known as fluorescence recovery after photobleaching (FRAP). In this process, the whole lens is first immersed in a bath of fluorescing molecules and left to soak for more than an hour, which allows the molecules to diffuse into the lens capsule and to ensure that the whole system is in chemical and diffusional equilibrium. Some of the molecules within the scaffold remain free to diffuse around in the medium and some become bound to the scaffold. The proportion in each of these “compartments”, and the affinity of the molecules for the scaffold, depends on their chemistry (*e.g.*, size, charge, etc.).

A high-intensity blue laser is used to bleach out a 5 μm radius tunnel through the capsule, creating a region of interest (ROI). The laser is focused at a plane within the capsule and, while the bleaching is most effective at this plane, bleaching occurs throughout the tunnel. After 250 ms, the laser is turned down to a very low intensity and used to take photographs of the focal circle. After the bleaching, a proportion of the cells within the 5 μm circle have stopped fluorescing, and the photographs show how the intensity of fluorescence increases with time as molecules from outside the circle diffuse in. The average intensity in the circle is calculated by counting up intensity of each of the pixels in the circle and dividing by the area. However, the amount of fluorescence decreases with time, so the fluorescence is also calculated over an identical “unbleached” region 50 μm away from the ROI, and the data in the ROI can be normalized by dividing by these data at each time.

Currently, the post-experiment data processing involves the following recipe. First, the normalized data is plotted and fitted with either

$$I = I_0 + I_1 \exp\left(-\frac{t}{\tau_{1/2}}\right) \quad \text{or} \quad I = I_0 + I_1 \exp\left(-\frac{t}{\tau_{1/2}^{(1)}}\right) + I_2 \exp\left(-\frac{t}{\tau_{1/2}^{(2)}}\right), \quad (1.1)$$

where they treat *all* the parameters in (1.1) as independent. Unsurprisingly, the “double exponential fit” with 5 independent fitting parameters fits the data better than the “single exponential” with 3 parameters (see Figure 1.2). After $\tau_{1/2}$ has been determined, the diffusivity is calculated using

$$D = \frac{\tilde{\omega}^2 \gamma_D}{4\tau_{1/2}}$$

(taken from a paper by Axelrod, *et al.*), where $\tilde{\omega}$ is the radius of the region of interest and $\gamma_D = 0.88$ is a “correction coefficient” used to take account of the radial geometry. There are two types of behavior exhibited by the kind of molecules used in the experiments, as illustrated below.

In Figure 1.3, the intensity curve tends to a steady state over the time scale of the experiment. This graph is associated with molecules that are tightly bound to the scaffold (and cannot leave).

In Figure 1.4, after the initial exponential transient, the intensity slowly increases back to its original value. This graph is associated with experiments where the bound molecules are exchanging with unbound ones.

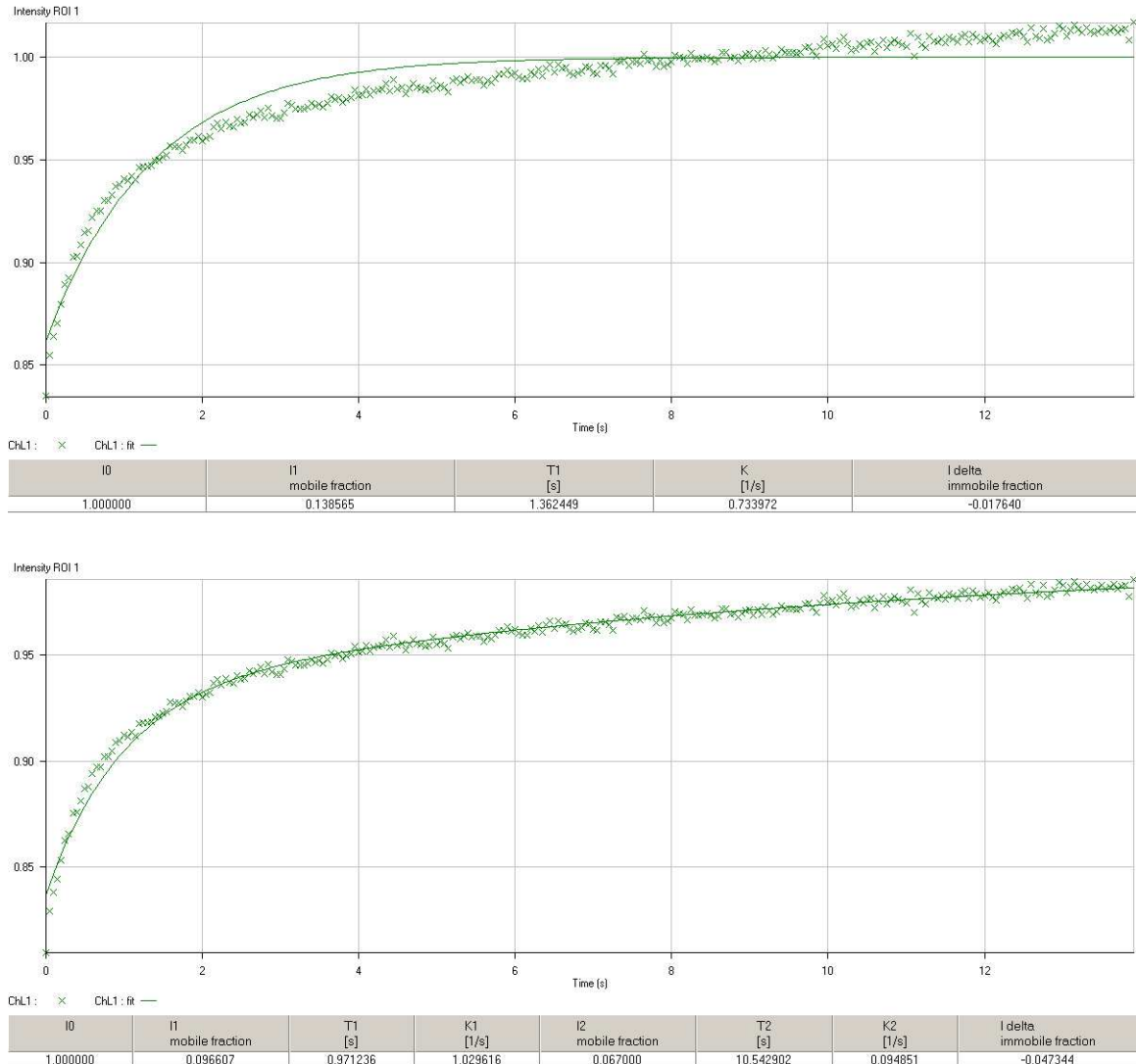


Figure 1.2. Experimental data with curve fit. Above: single exponential.
Below: double exponential.

The experimentalists are concerned with the procedures they use to interpret the data. Firstly, they are worried about the fact that they neglect all the influence of the third dimension, assuming that diffusion occurs only in a plane with no z -axis influence. Secondly, they are worried about whether the bleaching creates an aurora at the edge of the ROI which would alter their results. Thirdly, they are worried about when to truncate their time series and to fit the data: they find that truncating their data 10 s later can alter the fit parameters by 10%.

There are also concerns about how the data is normalized. During the actual experimental run, two regions are imaged: the bleached region and a control region. In an ideal situation, these two regions would have the same properties before the experiment, and only after bleaching would the readings diverge. Unfortunately, due to the random nature of the porous matrix, as well as varying optical properties of the device, the bleaching is not the same in both areas. (See Figure 1.5, which shows raw intensity data taken at the

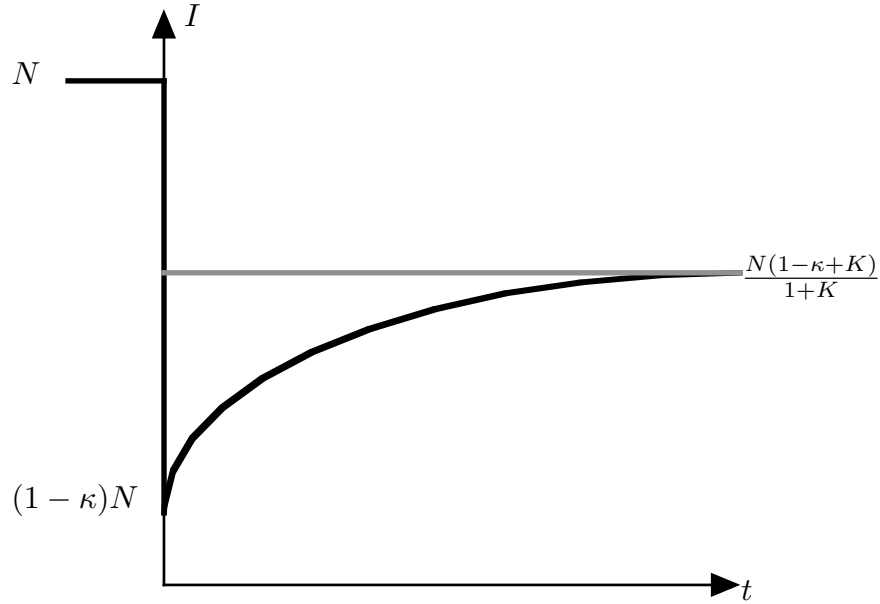


Figure 1.3. Schematic of intensity plot without kinetics.

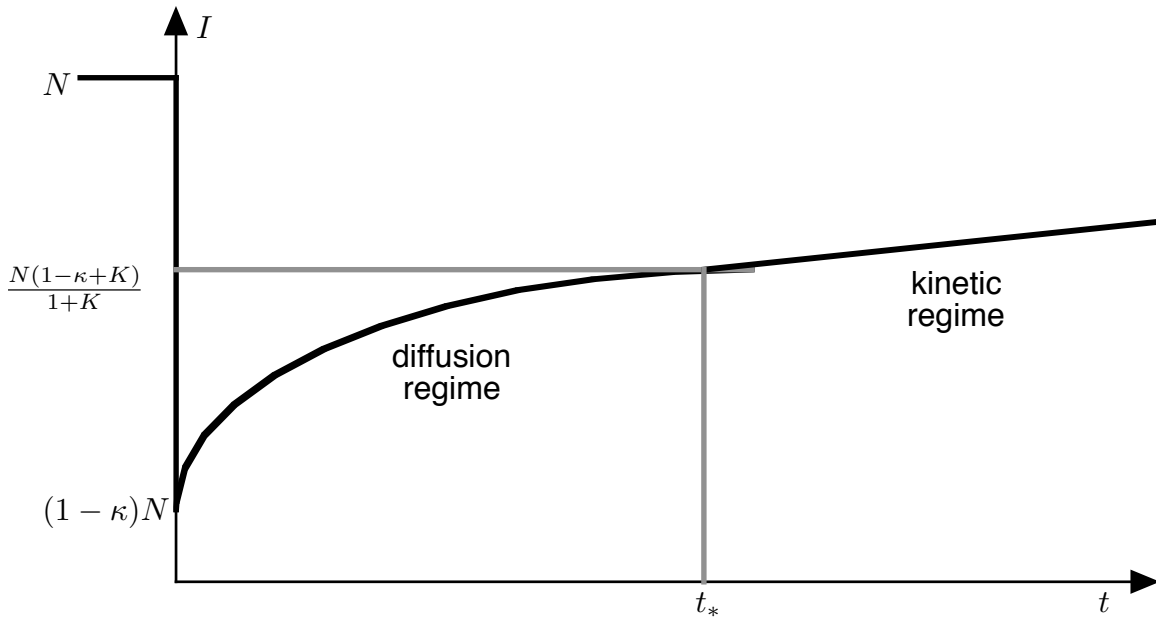


Figure 1.4. Schematic of intensity plot with kinetics.

same time).

We expect the porous matrix and the optical properties of the device to remain constant over the experiment, and to vary only spatially. If true, then we could normalize the measured data by the control region at time $t = 0$ as follows:

$$I(t) = \frac{I_{\text{control}}(0)}{I_{\text{bleached}}(0)} I_{\text{bleached}}(t).$$

Obviously, $I(0) = I_{\text{control}}(0)$. Since we don't expect the matrix to change over time, in

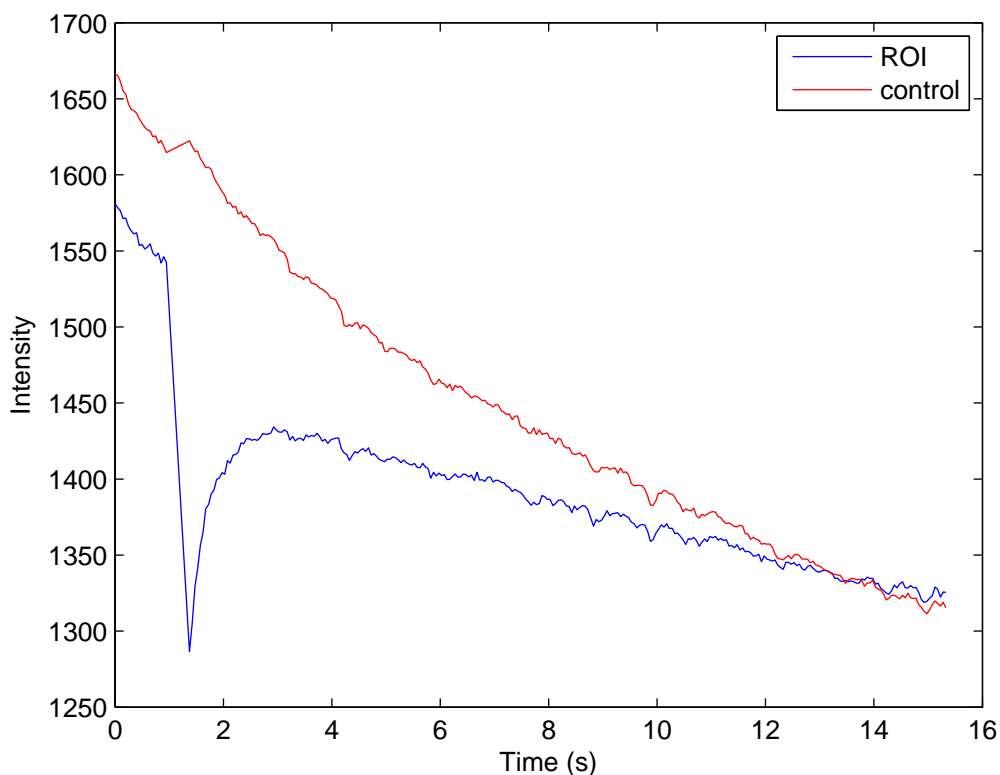


Figure 1.5. Raw intensity data. Top: control region. Bottom: bleached region.

theory this normalization should result in data which can be compared across experiments. Also, note that we expect the scaled control and bleached data to converge as $t \rightarrow \infty$. Unfortunately, this doesn't happen, as shown in Figure 1.6.

In the rest of this report we tackle the following questions:

1. Why does the double exponential fit better than the single exponential?
2. Why does the time at which you terminate the data alter the predictions?
3. Is there a more robust way to fit the data than is currently being used?
4. Does the effect of transfer between the mobile molecules and the bound ones explain the difference between the two types of graphs?

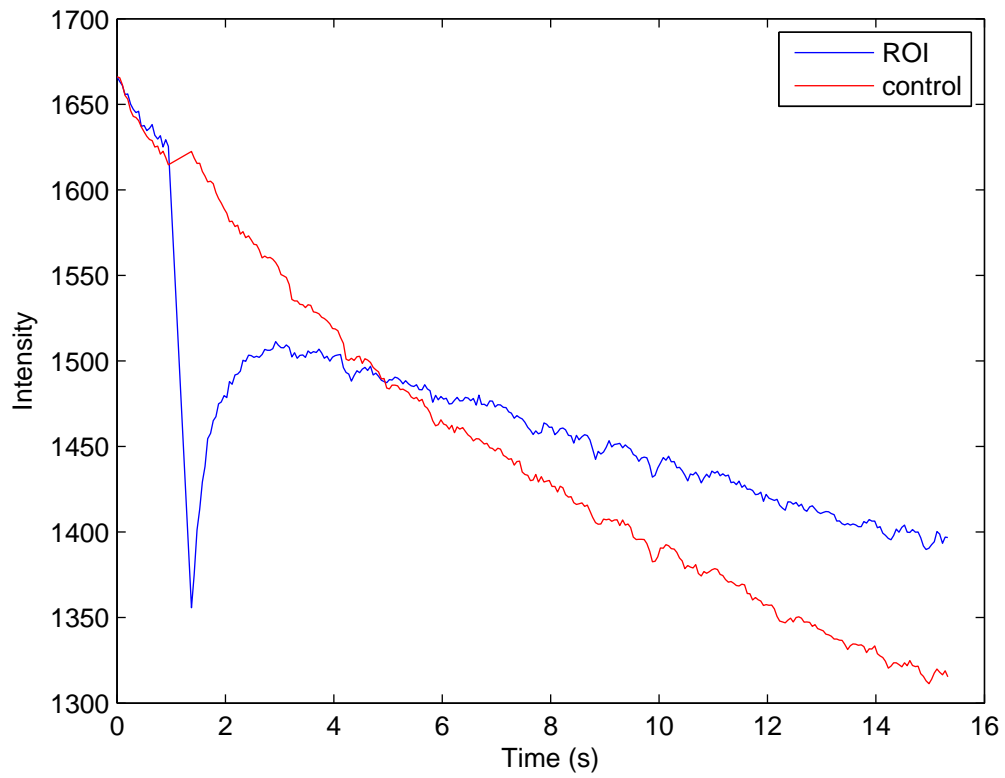


Figure 1.6. Scaled intensity curves. The graph with the initial dip is the bleached region; the other is the control region.

Section 2: Mathematical Model

At the beginning of the experiment, the membrane is saturated with fluorescing particles, and allowed to come to equilibrium. Then bleaching occurs in the ROI, which we consider to be a disk of radius $\tilde{\omega}$. We consider the bleaching to be radially symmetric. After bleaching, the measurement phase begins. We take $t = 0$ to be the time at which bleaching occurs. Therefore, we consider the end of the preparation phase to be $t = 0^-$.

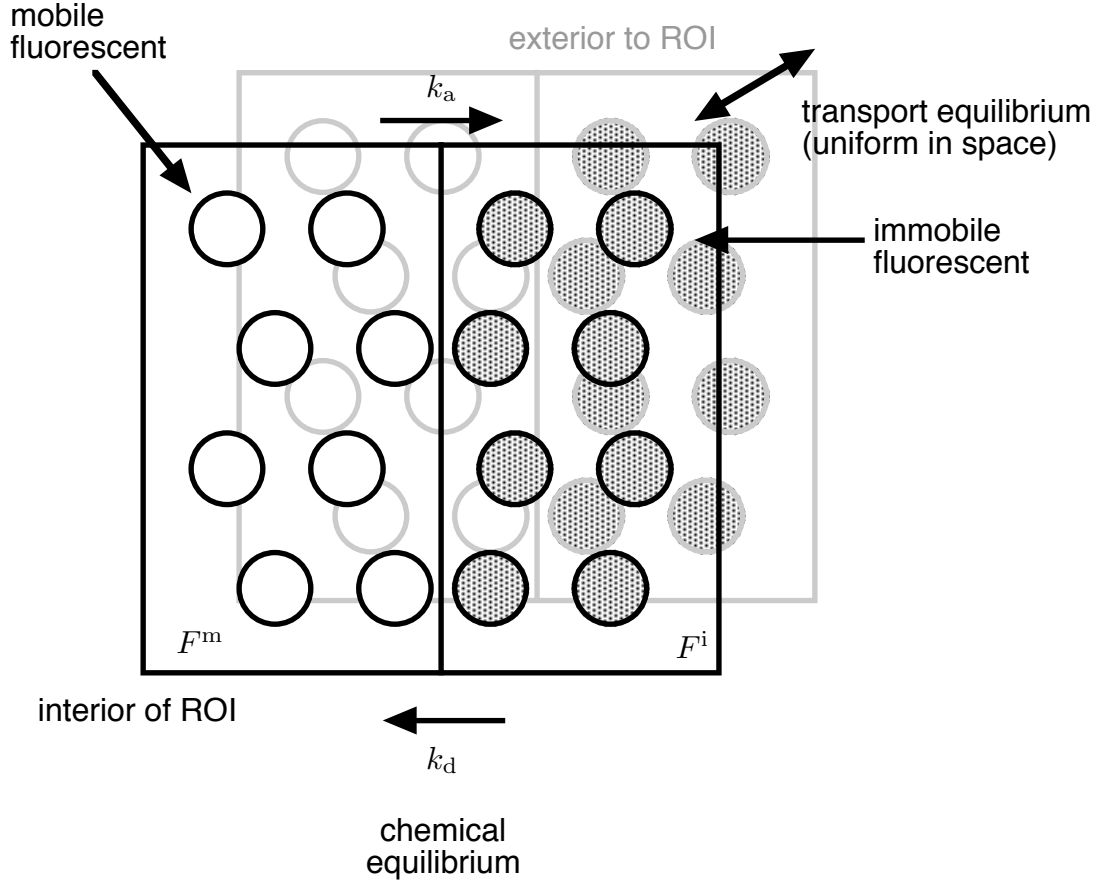


Figure 2.1. Schematic of experimental setup, $t = 0^-$.

The fluorescing particles come in two varieties: immobilized molecules which have attached to the membrane (with concentration F^i), which do not diffuse, and mobile molecules (with concentration F^m). (See Figure 2.1.) The particles are in *transport equilibrium*, so there is no average motion and hence the particles are uniformly distributed throughout the membrane:

$$F^i + F^m = N, \quad \tilde{r} > 0, \quad t = 0^-, \quad (2.1)$$

where N is the (constant) number of particles and we have chosen the spatial variable to be \tilde{r} , since the ROI is circular. (Though we argue on physical grounds in this section, the results can be established mathematically.)

The particles are also in “chemical equilibrium”, so the binding reaction (which we assume to follow simple mass-action kinetics) is in steady state. We assume that there are enough binding sites so that depletion is never an issue. Since the immobile species cannot diffuse, its evolution equation is given by

$$\frac{\partial F^i}{\partial t} = k_a F^m - k_d F^i, \quad (2.2)$$

where k_a is the rate constant for the association kinetics, and k_d is the rate constant for the dissociation kinetics. (Note that k_a as defined includes the concentration of the undepleted bulk, and so is somewhat nonstandard.) Since the preparation phase has been allowed to proceed to steady state before bleaching commences, we have the following:

$$k_a F^m = k_d F^i, \quad r > 0, \quad t = 0^-, \quad (2.3a)$$

$$F^m = K F^i, \quad K = \frac{k_d}{k_a}, \quad (2.3b)$$

where K is the *affinity constant*.

Combining (2.1) and (2.3b), we obtain at $t = 0^-$,

$$F^i(1 + K) = N$$

$$F^i(\tilde{r}, 0^-) = \frac{N}{1 + K}, \quad \tilde{r} > 0, \quad (2.4a)$$

$$F^m(\tilde{r}, 0^-) = \frac{NK}{1 + K}, \quad \tilde{r} > 0. \quad (2.4b)$$

At the beginning of the measurement phase, a laser beam bleaches some fraction of the fluorescent particles inside the ROI, permanently removing their fluorescent properties (see Figure 2.2). For the purposes of this section, we assume that

1. The bleaching process is uniform in space, bleaching a constant fraction κ of the fluorescent molecules. (In practice, $0.03 \leq \kappa \leq 0.2$.)
2. The bleaching process is taken to be faster than any other process in the problem, so it may be considered as instantaneous. The concentration of bleached particles will be denoted by B .

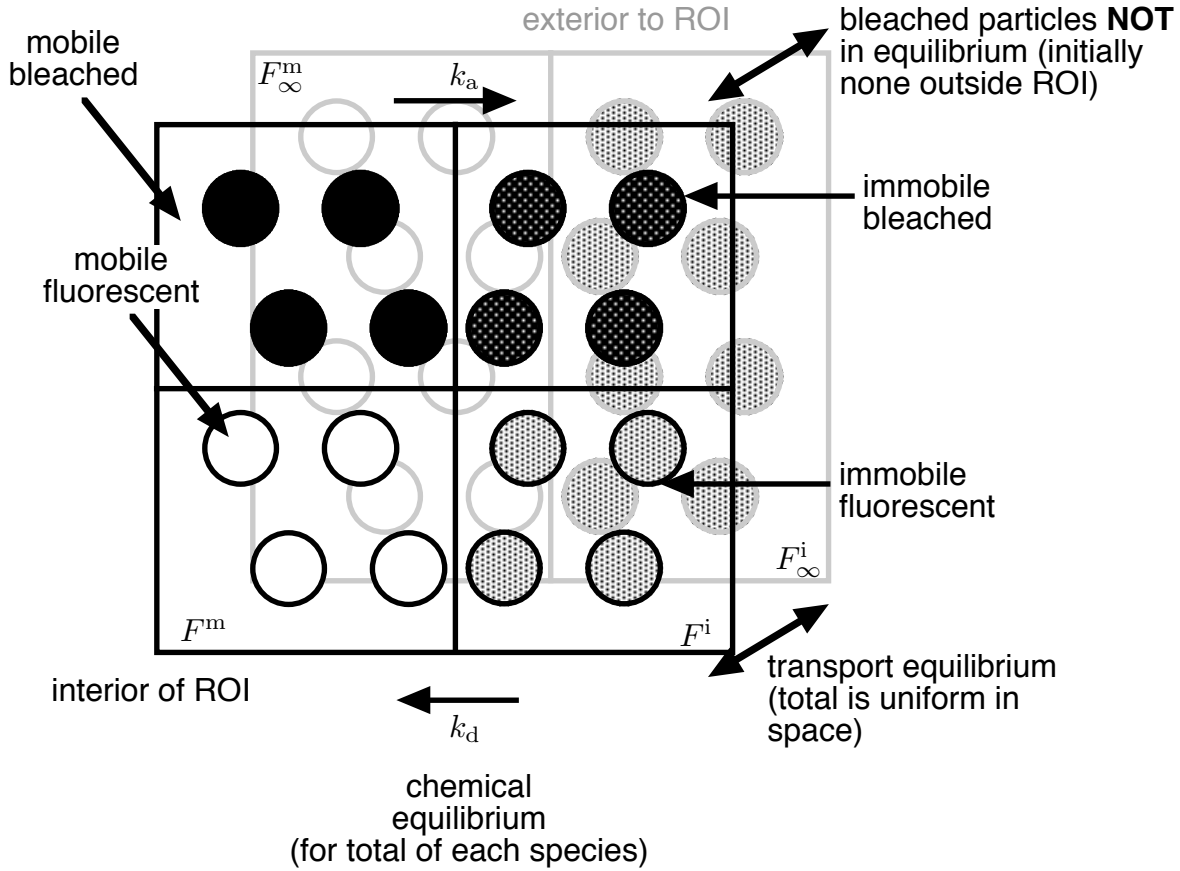
(Both of these assumptions will be relaxed in section 4.)

Then from (2.4) we see that initially we have the following in the region of interest:

$$F^i(\tilde{r}, 0^+) = \frac{N(1 - \kappa)}{1 + K} \equiv F_0^i, \quad 0 < \tilde{r} < \tilde{\omega}, \quad (2.5a)$$

$$F^m(\tilde{r}, 0^+) = \frac{NK(1 - \kappa)}{1 + K} \equiv F_0^m, \quad 0 < \tilde{r} < \tilde{\omega}. \quad (2.5b)$$

Note that we are changing only the labeling; the transport and chemical properties are unaffected. Therefore, (2.4) holds for all $t > 0$ as long as we consider the fluorescing


 Figure 2.2. Schematic of experimental setup, $t = 0^+$.

and bleached immobile or mobile molecules together, and hence we write:

$$F^i(\tilde{r}, t) + B^i(\tilde{r}, t) = \frac{N}{1 + K}, \quad (2.6a)$$

$$F^m(\tilde{r}, t) + B^m(\tilde{r}, t) = \frac{NK}{1 + K}. \quad (2.6b)$$

The light intensity is proportional to the number of fluorescent molecules, so we can use intensity and concentration interchangeably. The measured intensity $I(t)$ is simply the average over the ROI of all the fluorescing species F :

$$I(t) = \frac{1}{\pi\tilde{\omega}^2} \int_0^{\tilde{\omega}} \tilde{r} \int_0^{2\pi} F(\tilde{r}, \theta, t) d\theta d\tilde{r} = \frac{2}{\tilde{\omega}^2} \int_0^{\tilde{\omega}} \tilde{r} [F^i(\tilde{r}, t) + F^m(\tilde{r}, t)] d\tilde{r}, \quad (2.7)$$

where we have exploited the radial symmetry of the problem. Substituting (2.4) and (2.5) into (2.7), we have

$$I(0^-) = N, \quad (2.8a)$$

$$I(0^+) = (1 - \kappa)N. \quad (2.8b)$$

Section 3: 1 Compartment, No Kinetics

We begin by examining the case where the reactions take place on a time scale much slower than diffusion: mathematically, this means that

$$k_a \ll \frac{D}{r_\infty^2}, \quad k_d \ll \frac{D}{r_\infty^2},$$

where r_∞ is a characteristic radius defined below. Without kinetics included, the equation governing the evolution of F^m is

$$\frac{\partial F^m}{\partial t} = \frac{D}{\tilde{r}} \frac{\partial}{\partial \tilde{r}} \left(\tilde{r} \frac{\partial F^m}{\partial \tilde{r}} \right), \quad (3.1)$$

where D is the diffusion coefficient. We do not bother tracking the concentration of the bleached molecules, since they can be determined using (2.6b).

In order to solve the problem, we need boundary conditions on the various species. Clearly, they all must be bounded at $\tilde{r} = 0$. We then specify that at some distance $\tilde{r} = r_\infty$, the lens will transport any needed particles to and from the boundary very quickly. Therefore, we may specify Dirichlet data there that is specified by the preparation phase in (2.4), since we are outside the bleaching zone:

$$F^i(r_\infty, t) = \frac{N}{1 + K} \equiv F_\infty^i, \quad (3.2a)$$

$$F^m(r_\infty, t) = \frac{NK}{1 + K} \equiv F_\infty^m, \quad (3.2b)$$

where the subscript ∞ is used to reinforce that we are considering the exterior of the region $0 < \tilde{r} < r_\infty$ to be an infinite reservoir.

The form of (3.2) motivates the following scaling for \tilde{r} :

$$\tilde{r} = r_\infty r. \quad (3.3)$$

Substituting (3.3) into (3.1) and (3.2), we obtain

$$\frac{\partial F^m}{\partial t} = \frac{D}{r_\infty^2 r} \frac{\partial}{\partial r} \left(r \frac{\partial F^m}{\partial r} \right), \quad 0 < r < 1, \quad (3.4)$$

$$F^i(1, t) = \frac{N}{1 + K} \equiv F_\infty^i. \quad (3.5a)$$

$$F^m(1, t) = \frac{NK}{1 + K} \equiv F_\infty^m, \quad (3.5b)$$

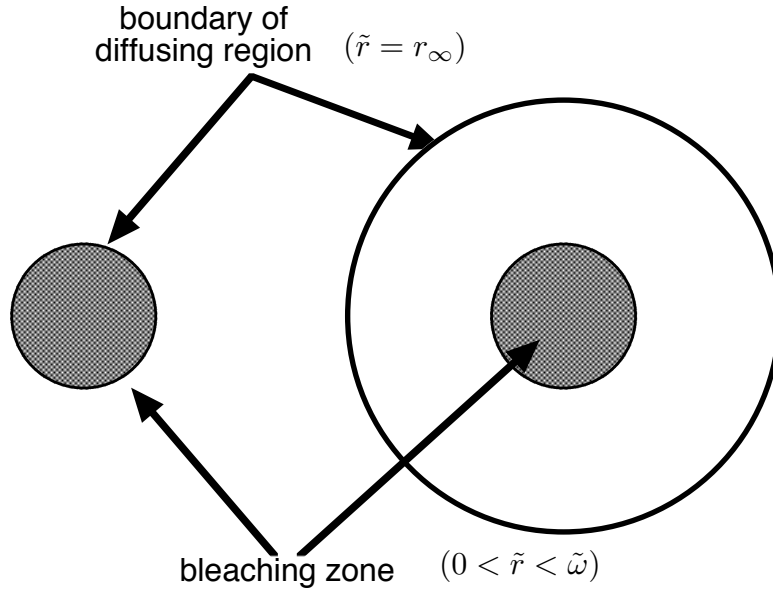


Figure 3.1. Left: one-compartment model. Right: two-compartment model.

Note that (3.4) is somewhat nonstandard in that r is dimensionless, but t is not. (Here we are being somewhat sloppy by using the same dependent variable notation.)

In this section we consider a *one-compartment* model (see left of Figure 3.1); that is, we take $r_\infty = \tilde{\omega}$, so the ROI becomes $0 \leq r \leq 1$ and (2.7) becomes

$$I(t) = 2 \int_0^1 r [F^i(r, t) + F^m(r, t)] dr. \quad (3.6)$$

In this case, F^i remains at its initial value given in (2.5a), so

$$I(t) = F_0^i + 2 \int_0^1 r F^m(r, t) dr. \quad (3.7)$$

To transform to homogeneous end conditions, we let

$$u^m(r, t) = F^m(r, t) - F_\infty^m \quad (3.8)$$

and then substitute this expression into (3.4), (2.5b), and (3.5b) to obtain

$$\frac{\partial u^m}{\partial t} = \frac{D}{r_\infty^2 r} \frac{\partial}{\partial r} \left(r \frac{\partial u^m}{\partial r} \right), \quad 0 \leq r \leq 1, \quad (3.9a)$$

$$u^m(1, t) = 0, \quad u^m(r, 0) = F_0^m - F_\infty^m = -\kappa F_\infty^m. \quad (3.9b)$$

Separating variables by setting $u^m(r, t) = R(r)T(t)$, we have the following:

$$RT' = \frac{DT(rR)'}{rr_\infty^2}$$

$$\frac{T'}{T} = \frac{D(rR)'}{rRr_\infty^2} = -\lambda.$$

Hence the equation for R is given by

$$rR'' + R' + \frac{\lambda r_\infty^2}{D} rR = 0, \quad R(1) = 0, \quad R(0) < \infty, \quad (3.10)$$

which has the solution

$$R_n(r) = J_0(j_{0,n}r), \quad (3.11a)$$

where $j_{0,n}$ is the n th zero of J_0 and

$$\lambda_n = \frac{Dj_{0,n}^2}{r_\infty^2}. \quad (3.11b)$$

Then solving the T equation, we obtain

$$\begin{aligned} T' + \lambda_n T &= 0 \\ T_n(t) &= T_n(0) \exp(-\lambda_n t). \end{aligned} \quad (3.12)$$

Then by the principle of superposition, we have that

$$u^m(r, t) = -F_\infty^m \sum_{n=1}^{\infty} T_n(0) J_0(j_{0,n}r) \exp(-\lambda_n t), \quad (3.13)$$

where by the orthogonality properties of the Bessel function we have the following:

$$T_n(0) = \left[\kappa \int_0^1 r J_0(j_{0,n}r) dr \right] \left[\int_0^1 r J_0^2(j_{0,n}r) dr \right]^{-1}. \quad (3.14)$$

For later calculations, it will be useful to define

$$\int_0^1 r f(r) J_0(j_{0,n}r) dr \equiv a_n(f), \quad (3.15)$$

for any function f . Hence the first bracketed expression in (3.14) may be replaced by $\kappa a_n(1)$ and we have

$$\begin{aligned} T_n(0) &= \kappa a_n(1) \left[\frac{1}{2} J_1^2(j_{0,n}) \right]^{-1} = \frac{2[\kappa a_n(1)]}{J_1^2(j_{0,n})}, \\ a_n(1) &= \int_0^1 r J_0(j_{0,n}r) dr = \frac{1}{j_{0,n}^2} \int_0^{j_{0,n}} \rho J_0(\rho) d\rho = \left[\frac{\rho J_1(\rho)}{j_{0,n}^2} \right]_0^{j_{0,n}} \\ &= \frac{J_1(j_{0,n})}{j_{0,n}}. \end{aligned} \quad (3.16)$$

The relationship for the norm of J_0 is given by Theorem 4.23 in Bell (1968), while the integral in $a_n(1)$ is given by Theorem 4.8(i) in Bell (1968).

Substituting (3.14) into (3.13) and using (3.8), we obtain

$$u^m(r, t) = -F_\infty^m \sum_{n=1}^{\infty} \frac{2[\kappa a_n(1)]}{J_1^2(j_{0,n})} J_0(j_{0,n}r) \exp(-\lambda_n t), \quad (3.17a)$$

$$F^m(r, t) = F_\infty^m - F_\infty^m \sum_{n=1}^{\infty} \frac{2[\kappa a_n(1)]}{J_1^2(j_{0,n})} J_0(j_{0,n}r) \exp(-\lambda_n t). \quad (3.17b)$$

(We do not perform further simplification at this time because the general form of (3.17) will be used in later sections.) Note from (3.17b) that $F^m(r, \infty) = F_\infty^m$, as expected, and thus the concentration returns to its bulk value. Therefore, we have that

$$I(\infty) = F_0^i + F_\infty^m = \frac{N(1 - \kappa)}{1 + K} + \frac{NK}{1 + K} = \frac{N(1 - \kappa + K)}{1 + K}, \quad (3.18)$$

where we have used (2.5a) and (3.5b).

Using the definitions in (2.5) and (3.5) in (3.7), we have the following:

$$I(t) = \frac{(1 - \kappa)N}{1 + K} + \frac{KN}{1 + K} - \frac{NK}{1 + K} \sum_{n=1}^{\infty} \frac{2[\kappa a_n(1)]}{J_1^2(j_{0,n})} \exp(-\lambda_n t) \left[2 \int_0^1 r J_0(j_{0,n}r) dr \right] \quad (3.19a)$$

$$= \frac{(1 - \kappa + K)N}{1 + K} - \frac{2NK}{1 + K} \sum_{n=1}^{\infty} \frac{[\kappa a_n(1)][2a_n(1)]}{J_1^2(j_{0,n})} \exp(-\lambda_n t), \quad (3.19b)$$

where we have used (3.7). Here we have left (3.19b) unsimplified to facilitate further extensions in the next section. However, substituting in (3.16) for this case, we obtain

$$I(t) = \frac{(1 - \kappa + K)N}{1 + K} - \frac{4\kappa NK}{1 + K} \sum_{n=1}^{\infty} \frac{\exp(-\lambda_n t)}{j_{0,n}^2}. \quad (3.20)$$

There are four parameters to be determined in this problem. Two of these parameters, N and κ , can be determined from the data at $t = 0^\pm$. In particular, N can be determined from the intensity plot at the end of the saturation phase ($t = 0^-$) as shown in (2.8a), and κ can be determined at the beginning of the measurement phase ($t = 0^+$) as shown in (2.8b). Note that this simplification is not immediately visible from (3.20), though it can be readily established once one recalls that

$$\sum_{n=1}^{\infty} \frac{1}{j_{0,n}^2} = \frac{1}{4}.$$

The remaining two parameters, D and K , must be determined by fitting the shape of the curve. A good starting guess for K can be determined by looking at the long-term asymptote of the data, as can be seen from (3.18). (What constitutes “long-term” is not a trivial matter, and will be discussed more in the conclusion.) The effect of D in the

solution is manifested through λ_n , as shown in (3.11b). Thus D can be determined only from the behavior of the curve in the evolution phase. Note that the most complicated part of the problem, the $j_{0,n}$, may be calculated once and stored in a table.

During the workshop, a Matlab implementation of (3.20) was written. N and κ were estimated directly from the data, and the values substituted into (3.20). The resulting sum was fit (with 25 terms) against the data to determine D and K . The optimization for D was always started with $D = 1 \mu\text{m}^2/\text{s}$, as this is a common order-of-magnitude estimate. Four starting values of K were used, and the code runs four optimizations using each value. Two graphs are shown below.

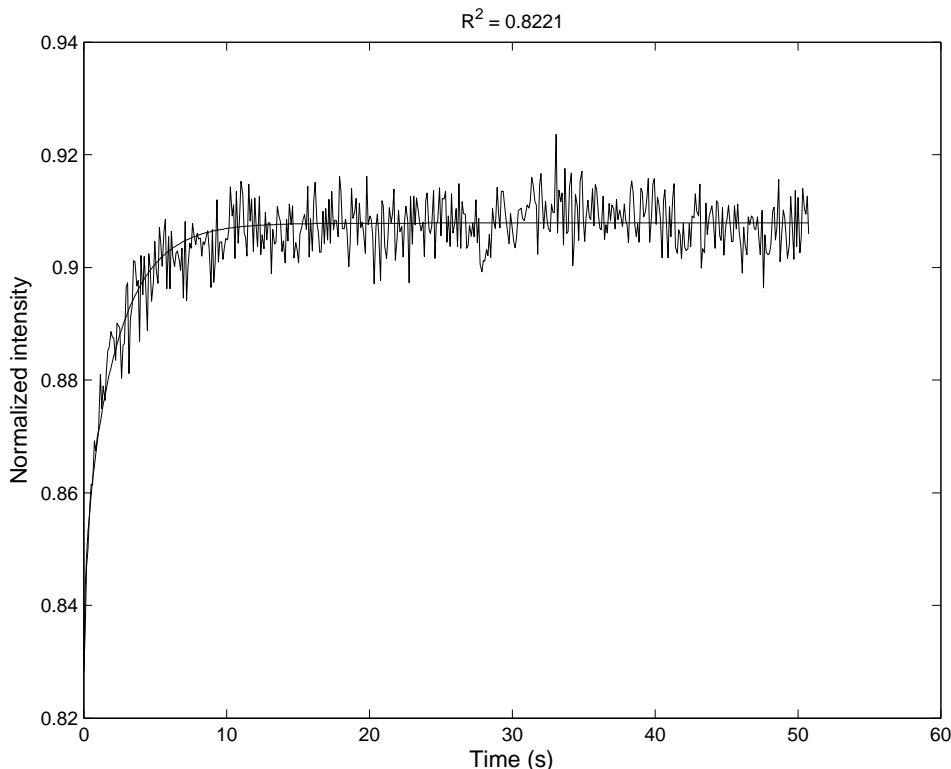


Figure 3.2. Data without obvious kinetic effects.

Figure 3.2 shows data from an anionic dextran molecule of size 40 kDa. (Here the “ R^2 ” at the top of the graph refers to the statistical goodness-of-fit test.) We see that the data roughly matches the schematic in Figure 1.3, namely, there is a noticeable steady state in the data, which we expect should make it a good candidate for the model presented in this section. This is borne out by the good fit for the curve; the key parameters obtained are

$$D = 1.748 \frac{\mu\text{m}^2}{\text{s}}, \quad K = 26.52. \quad (3.21)$$

Figure 3.3 shows data from a cationic dextran molecule of size 10 kDa. We see that the data roughly matches the schematic in Figure 1.4. Namely, there seems to be slow linear growth in the data for long time. Hence we expect kinetics to play a role, and for

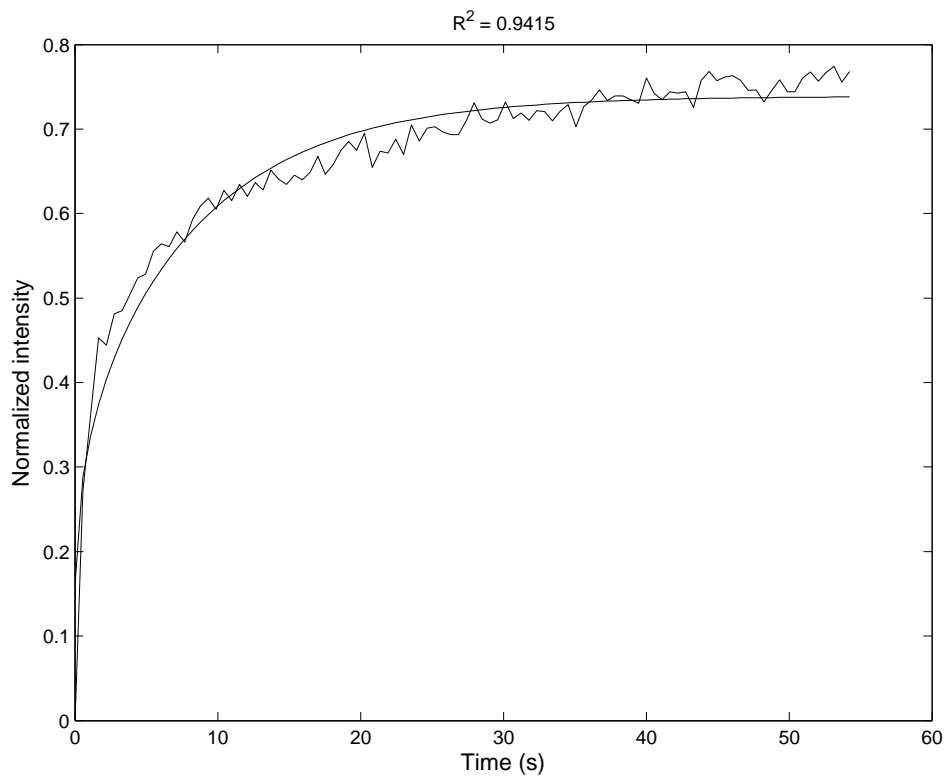


Figure 3.3. Data not explained with kinetic-free model.

the model presented in this section to not work well. This is borne out by the bad fit for the curve; the key parameters obtained are

$$D = 0.490428 \frac{\mu\text{m}^2}{\text{s}}, \quad K = 2.22997. \quad (3.22)$$

Section 4: Extensions

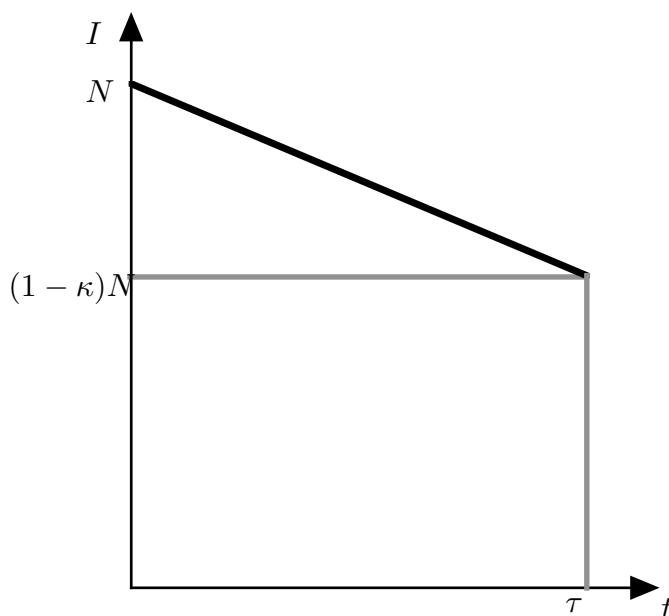


Figure 4.1. Schematic of bleaching over time.

Fast Diffusion

In some cases, bleaching takes place on a time scale roughly equal to that for diffusion. Hence the bleaching process cannot be taken to be instantaneous. For simplicity, we model the bleaching as a linear process over some time interval τ (see Figure 4.1. This was later determined to be an erroneous assumption; see section 7.)

Therefore, we see that in the absence of diffusion, we would have

$$\frac{d(F^i + F^m)}{dt} = \frac{N(1 - \kappa) - N}{\tau} = -\frac{N\kappa}{\tau}, \quad 0 < t < \tau. \quad (4.1)$$

We now make a further simplifying assumption. We assume that the bleaching affects each category (mobile and immobile) of fluorescent molecules in proportion to their equilibrium concentration fraction. Then since the immobile molecules cannot move, we have that

$$\frac{dF^i}{dt} = -\frac{N\kappa}{\tau(1 + K)}, \quad 0 < t < \tau, \quad (4.2)$$

from which we obtain the following:

$$\begin{aligned} F^i &= \frac{N}{(1 + K)} - \frac{N\kappa t}{\tau(1 + K)} = \frac{N}{1 + K} \left(1 - \frac{\kappa t}{\tau}\right) \\ &= F_\infty^i \left(1 - \frac{\kappa t}{\tau}\right), \quad 0 < t < \tau, \\ F^i &= \frac{N(1 - \kappa)}{1 + K} = F_0^i, \quad t > \tau, \end{aligned} \quad (4.3)$$

where we have used (3.2a). Then combining (4.1) and (4.2), we see that in the absence of diffusion, the contribution to the evolution of F^m from the bleaching must be

$$\frac{dF^m}{dt} = -\frac{NK\kappa}{\tau(1+K)} = -\frac{\kappa F_\infty^m}{\tau}, \quad 0 < t < \tau.$$

We note that the initial and boundary conditions for this problem must be the same because bleaching has not begun when $t = 0$. Therefore, in this situation, (3.9) becomes

$$\frac{\partial u^m}{\partial t} = \frac{D}{r_\infty^2 r} \frac{\partial}{\partial r} \left(r \frac{\partial u^m}{\partial r} \right) - \frac{\kappa F_\infty^m}{\tau}, \quad 0 \leq r \leq 1, \quad 0 \leq t \leq \tau, \quad (4.4a)$$

$$u^m(1, t) = 0, \quad u^m(r, 0) = 0. \quad (4.4b)$$

Motivated by (3.17a), we solve (4.4a) *via* the following eigenfunction expansion (Fourier-Bessel series):

$$u^m(r, t) = \sum_{n=1}^{\infty} \frac{2}{J_1^2(j_{0,n})} T_n^m(t) J_0(j_{0,n}r), \quad T_n^m(t) = \int_0^1 r u^m(r, t) J_0(j_{0,n}r) dr. \quad (4.5)$$

We note that this is not the standard form; normally the normalization factor $2/J_1^2(j_{0,n})$ would multiply the integral term. Substituting (4.5) into (4.4), we obtain

$$\frac{dT_n^m}{dt} = -\lambda_n T_n^m - \frac{\kappa F_\infty^m a_n(1)}{\tau}, \quad T_n^m(0) = 0,$$

where λ_n is given by (3.11b). Now we see that the choice of terms in (4.5) allowed the forcing term to be written in terms of the previously defined $a_n(1)$. Solving the above for $t < \tau$, we obtain

$$T_n^m(t) = -\frac{\kappa F_\infty^m a_n(1)}{\tau \lambda_n} [1 - \exp(-\lambda_n t)], \quad 0 < t < \tau. \quad (4.6a)$$

The bleaching process ends at $t = \tau$. Therefore, for $t > \tau$, the system is governed by the equations in section 3. In particular, from (3.12) we have that $T_n(t)$ is a simple decaying exponential that must match to (4.6a) at $t = \tau$, so we have the following:

$$T_n^m(t) = -\frac{\kappa F_\infty^m a_n(1)}{\tau \lambda_n} [1 - \exp(-\lambda_n \tau)] \exp(-\lambda_n(t - \tau)), \quad t > \tau. \quad (4.6b)$$

Note that

$$\lim_{\tau \rightarrow 0} T_n^m = -\kappa F_\infty^m a_n(1) \exp(-\lambda_n t),$$

which agrees with (3.17a) (*i.e.*, the limiting case of instantaneous bleaching reduces to the case in section 3).

Since we are changing only the time-dependent part, we see that (3.19b) and (3.20) become

$$I(t) = \begin{cases} \frac{(1 - \kappa + K)N}{1 + K} - \frac{2NK}{1 + K} \sum_{n=1}^{\infty} \frac{[\kappa a_n(1)][2a_n(1)]}{J_1^2(j_{0,n})} \frac{1 - \exp(-\lambda_n t)}{\tau \lambda_n}, & 0 < t < \tau, \\ \frac{(1 - \kappa + K)N}{1 + K} - \frac{2NK}{1 + K} \sum_{n=1}^{\infty} \frac{[\kappa a_n(1)][2a_n(1)]}{J_1^2(j_{0,n})} \frac{1 - \exp(-\lambda_n \tau)}{\tau \lambda_n} \exp(-\lambda_n(t - \tau)), & t > \tau, \end{cases} \quad (4.7a)$$

$$I(t) = \begin{cases} \frac{(1 - \kappa + K)N}{1 + K} - \frac{4\kappa NK}{1 + K} \sum_{n=1}^{\infty} \frac{1 - \exp(-\lambda_n t)}{\tau \lambda_n j_{0,n}^2}, & 0 < t < \tau, \\ \frac{(1 - \kappa + K)N}{1 + K} - \frac{4\kappa NK}{1 + K} \sum_{n=1}^{\infty} \frac{1 - \exp(-\lambda_n \tau)}{\tau \lambda_n j_{0,n}^2} \exp(-\lambda_n(t - \tau)), & t > \tau. \end{cases} \quad (4.7b)$$

Non-Uniform Bleaching

In some cases, the bleaching may not be perfectly uniform. In that case, rather than κ being a constant, it will be a function of r . Thus the first bracketed term in (3.14) must be replaced by

$$\int_0^1 r \kappa(r) J_0(j_{0,n} r) dr = a_n(\kappa), \quad (4.8)$$

where we have used the notation in (3.15). This substitution carries through to the first bracketed term in (3.19b), so in this case we have

$$I(t) = \frac{(1 - \kappa + K)N}{1 + K} - \frac{2NK}{1 + K} \sum_{n=1}^{\infty} \frac{[a_n(\kappa)][2a_n(1)]}{J_1^2(j_{0,n})} \exp(-\lambda_n t) \quad (4.9a)$$

$$= \frac{(1 - \kappa + K)N}{1 + K} - \frac{4NK}{1 + K} \sum_{n=1}^{\infty} \frac{a_n(\kappa)}{j_{0,n} J_1(j_{0,n})} \exp(-\lambda_n t). \quad (4.9b)$$

Non-Uniform Sensing

In some cases, the sensing may not be perfectly uniform, but instead the signal strength S varies with r . In that case, we replace (3.6) with

$$I(t) = \frac{1}{S_*} \int_0^1 r S(r) [F^i(r, t) + F^m(r, t)] dr, \quad S_* = \int_0^1 r S(r) dr. \quad (4.10)$$

Here S_* is a normalization constant chosen to ensure that if $F^i(r, t) + F^m(r, t)$ is a constant, $I(t)$ will be that same constant. Thus the second bracketed term in (3.19a) must be replaced by

$$\frac{1}{S_*} \int_0^1 r S(r) J_0(j_{0,n} r) dr \equiv \frac{a_n(S)}{S_*}. \quad (4.11)$$

Thus (3.19b) becomes

$$I(t) = \frac{(1 - \kappa + K)N}{1 + K} - \frac{2NK}{1 + K} \sum_{n=1}^{\infty} \frac{[\kappa a_n(1)][a_n(S)/S_*]}{J_1^2(j_{0,n})} \exp(-\lambda_n t), \quad (4.12a)$$

$$= \frac{(1 - \kappa + K)N}{1 + K} - \frac{2\kappa NK}{S_*(1 + K)} \sum_{n=1}^{\infty} \frac{a_n(S)}{j_{0,n} J_1(j_{0,n})} \exp(-\lambda_n t). \quad (4.12b)$$

Two-Compartment Model

Since there is no change in the medium at the bleaching zone interface, there is no reason to suspect that the concentration should remain at a fixed value there. Therefore, we may introduce a *two-compartment* model by defining

$$\omega = \frac{\tilde{\omega}}{r_\infty}, \quad (4.13)$$

and not requiring that $\omega = 1$ (see right of Figure 3.1).

This then results in a combination of the previous two cases. If we take uniform bleaching within the zone, we have

$$\begin{aligned} \kappa(r) &= \kappa(1 - H(r - \omega)), \\ a_n(\kappa) &= \kappa \int_0^\omega r J_0(j_{0,n} r) dr = \frac{\kappa}{j_{0,n}^2} \int_0^{j_{0,n}\omega} \rho J_0(\rho) d\rho = \frac{\kappa J_1(j_{0,n}\omega)\omega}{j_{0,n}}, \end{aligned} \quad (4.14)$$

where H is the Heaviside function. Similarly, if we average uniformly within the zone, we obtain

$$S(r) = 1 - H(r - \omega),$$

which corresponds to no signal outside the ROI. Continuing to simplify, we obtain

$$a_n(S) = \frac{\omega J_1(j_{0,n}\omega)}{j_{0,n}}, \quad (4.15a)$$

$$S_* = \int_0^\omega r dr = \frac{\omega^2}{2}. \quad (4.15b)$$

Thus (3.19b) becomes

$$I(t) = \frac{(1 - \kappa + K)N}{1 + K} - \frac{2NK}{1 + K} \sum_{n=1}^{\infty} \frac{[a_n(\kappa)][a_n(S)/S_*]}{J_1^2(j_{0,n})} \exp(-\lambda_n t) \quad (4.16a)$$

$$= \frac{(1 - \kappa + K)N}{1 + K} - \frac{4\kappa NK}{1 + K} \sum_{n=1}^{\infty} \frac{J_1^2(j_{0,n}\omega)}{j_{0,n}^2 J_1^2(j_{0,n})} \exp(-\lambda_n t). \quad (4.16b)$$

Note that if $\omega = 1$ (which corresponds to the one-compartment model), (4.16b) reduces to (3.20).

The two-compartment model introduces a new parameter, ω , which must be determined. There are several ways to do this:

1. r_∞ can be chosen to be the radius of the lens (considered to be a cylinder pressed against the slide), since that is the maximal extent of the domain.
2. ω can be chosen arbitrarily, and the other parameters estimated for an experimental run. Then for the same experimental run, one may vary ω and do another fit. In this way, one can check the sensitivity of the dynamic parameters to the choice of ω .
3. ω can be fit directly. Once ω is found, then r_∞ may be determined since $\tilde{\omega}$ is known, and then D may be determined from the λ_n . However, note that this is much more computationally intensive, since each of the Bessel function coefficients must be recalculated with each iteration.

Obviously this formulation is inexact. One could think of taking $r_\infty \rightarrow \infty$ and solving the diffusion problem on the full two-dimensional space. But the solution of such a problem is of the form (Carslaw and Jaeger, 1959, 14.8(1))

$$F^m = \int_0^\infty \frac{f(\rho)}{4\pi Dt} \exp\left(-\frac{r^2 + \rho^2}{4Dt}\right) I_0\left(\frac{r\rho}{2Dt}\right) d\rho, \quad (4.17)$$

which is an infinite integral. This is similar to the approach taken by Sprague, *et al* (2004).

The final product of this report will be a Matlab code that will estimate the physical parameters given experimental data. In such a product, the infinite integral in (4.17) would have to be approximated by some quadrature on $[0, r_\infty]$ anyway. So that is why we retain the finite-interval formulation, and the solution form (4.16b).

Section 5: One Compartment With Kinetics

Next we treat the case with kinetics. In this case, the amount of F^m can be changed by binding or dissociation, so (3.4) is replaced by

$$\frac{\partial F^m}{\partial t} = \frac{D}{r_\infty^2 r} \frac{\partial}{\partial r} \left(r \frac{\partial F^m}{\partial r} \right) - k_a F^m + k_d F^i, \quad (5.1a)$$

which is coupled to (2.2), which we repeat here for clarity:

$$\frac{\partial F^i}{\partial t} = k_a F^m - k_d F^i. \quad (5.1b)$$

To obtain homogeneous end conditions for both dependent variables, as before we set

$$u^i(r, t) = F^i(r, t) - F_\infty^i, \quad u^m(r, t) = F^m(r, t) - F_\infty^m. \quad (5.2)$$

Substituting (5.2) into (5.1a), we obtain

$$\begin{aligned} \frac{\partial u^m}{\partial t} &= \frac{D}{r_\infty^2 r} \frac{\partial}{\partial r} \left(r \frac{\partial u^m}{\partial r} \right) - k_a (u^m + F_\infty^m) + k_d (u^i + F_\infty^i) \\ &= \frac{D}{r_\infty^2 r} \frac{\partial}{\partial r} \left(r \frac{\partial u^m}{\partial r} \right) - k_a u^m + k_d u^i, \end{aligned} \quad (5.3a)$$

where we have used the fact that (2.3a) holds for the bulk values. Similarly, (5.1b) becomes

$$\frac{\partial u^i}{\partial t} = -k_d u^i + k_a u^m, \quad (5.3b)$$

and the boundary conditions for u^i become

$$u^i(1, t) = 0, \quad u^i(r, 0) = F_0^i - F_\infty^i = -\kappa F_\infty^i. \quad (5.4)$$

Motivated by (4.5), we let

$$u^i(r, t) = - \sum_{n=1}^{\infty} \frac{2\kappa a_n(1) T_n^i(t)}{J_1^2(j_{0,n})} J_0(j_{0,n} r), \quad T_n^i(t) = - \frac{1}{\kappa a_n(1)} \int_0^1 r u^i(r, t) J_0(j_{0,n} r) dr. \quad (5.5)$$

Again, the choice of coefficients simplifies the algebra later on. In particular, we see that

$$T_n^i(0) = - \frac{1}{\kappa a_n(1)} \int_0^1 r (-\kappa F_\infty^i) J_0(j_{0,n} r) dr = F_\infty^i. \quad (5.6)$$

Simplifying the above and extending it to the other species, we obtain

$$u^i(r, t) = - \sum_{n=1}^{\infty} \frac{2\kappa T_n^i(t)}{J_1(j_{0,n})} \frac{J_0(j_{0,n}r)}{j_{0,n}}, \quad (5.7a)$$

$$u^m(r, t) = - \sum_{n=1}^{\infty} \frac{2\kappa T_n^m(t)}{J_1(j_{0,n})} \frac{J_0(j_{0,n}r)}{j_{0,n}}, \quad T_n^m(0) = F_{\infty}^m. \quad (5.7b)$$

Substituting (5.7) into (5.3), we obtain

$$\begin{aligned} \frac{dT_n^m}{dt} &= -\lambda_n T_n^m - k_a T_n^m + k_d T_n^i, \\ \frac{dT_n^i}{dt} &= -k_d T_n^i + k_a T_n^m, \end{aligned}$$

where we have used (3.11b). Rewriting the above in matrix form, we have

$$\frac{d}{dt} \begin{pmatrix} T_n^m \\ T_n^i \end{pmatrix} = A \begin{pmatrix} T_n^m \\ T_n^i \end{pmatrix}, \quad A = \begin{pmatrix} -\lambda_n - k_a & k_d \\ k_a & -k_d \end{pmatrix} \quad (5.8a)$$

$$\begin{pmatrix} T_n^m \\ T_n^i \end{pmatrix} = c_+ e^{\alpha_+ t} \mathbf{v}_+ + c_- e^{\alpha_- t} \mathbf{v}_-, \quad (5.8b)$$

Here (α, \mathbf{v}) are the eigenvalue-eigenvector pairs of A , given by

$$\begin{aligned} (\alpha + \lambda_n + k_a)(\alpha + k_d) - k_a k_d &= 0 \\ \alpha^2 + (\lambda_n + k_a + k_d)\alpha + k_d \lambda_n &= 0 \\ \alpha_{\pm} &= \frac{-(\lambda_n + k_a + k_d) \pm \sqrt{(\lambda_n + k_a + k_d)^2 - 4k_d \lambda_n}}{2}, \end{aligned} \quad (5.9a)$$

$$\mathbf{v}_{\pm} = \begin{pmatrix} k_d + \alpha_{\pm} \\ k_a \end{pmatrix}. \quad (5.9b)$$

The initial conditions for the problem are given by

$$\begin{pmatrix} T_n^m \\ T_n^i \end{pmatrix} (0) = c_+ \mathbf{v}_+ + c_- \mathbf{v}_- = \begin{pmatrix} F_{\infty}^m \\ F_{\infty}^i \end{pmatrix}.$$

Solving this equation for the c_{\pm} , we obtain

$$\begin{aligned} \begin{pmatrix} T_n^m \\ T_n^i \end{pmatrix} (0) &= c_+ \mathbf{v}_+ + c_- \mathbf{v}_- = \begin{pmatrix} F_{\infty}^m \\ F_{\infty}^i \end{pmatrix} \\ c_+(k_d + \alpha_+) + c_-(k_d + \alpha_-) &= F_{\infty}^m \\ c_+ k_a + c_- k_a &= F_{\infty}^i \\ c_+ k_d + c_- k_d &= F_{\infty}^m \end{aligned}$$

$$\begin{aligned}
c_+ \alpha_+ + c_- \alpha_- &= 0 \\
c_- \left(1 - \frac{\alpha_-}{\alpha_+}\right) &= \frac{F_\infty^m}{k_d} \\
c_- &= \frac{F_\infty^m \alpha_+}{k_d (\alpha_+ - \alpha_-)}, \tag{5.10a}
\end{aligned}$$

$$c_+ = -\frac{F_\infty^m \alpha_-}{k_d (\alpha_+ - \alpha_-)}. \tag{5.10b}$$

Note that as the rate constants go to zero, we have

$$A \rightarrow \begin{pmatrix} -\lambda_n & 0 \\ 0 & 0 \end{pmatrix}, \quad \alpha \rightarrow \{-\lambda_n, 0\}, \quad \mathbf{v} \rightarrow \{\mathbf{e}_1, \mathbf{e}_2\},$$

and we reduce to the no-kinetics case where T^i is a constant and T_n^m decays exponentially. Substituting our expressions into (3.6) to obtain the intensity, we obtain the following:

$$\begin{aligned}
I(t) &= F_\infty^i + F_\infty^m + 2 \int_0^1 r [u^i(r, t) + u^m(r, t)] dr \\
&= \frac{N}{1+K} + \frac{NK}{1+K} - 4\kappa \sum_{n=1}^{\infty} \frac{T_n^i(t) + T_n^m(t)}{j_{0,n} J_1(j_{0,n})} \int_0^1 r J_0(j_{0,n} r) dr \\
&= N - 4\kappa \sum_{n=1}^{\infty} \frac{c_+ e^{\alpha_+ t} (k_d + k_a + \alpha_+) + c_- e^{\alpha_- t} (k_d + k_a + \alpha_-)}{j_{0,n}^2} \tag{5.11a}
\end{aligned}$$

$$\begin{aligned}
&= N - \frac{4\kappa F_\infty^m}{k_d} \sum_{n=1}^{\infty} \frac{-\alpha_- e^{\alpha_+ t} (k_d + k_a + \alpha_+) + \alpha_+ e^{\alpha_- t} (k_d + k_a + \alpha_-)}{j_{0,n}^2 (\alpha_+ - \alpha_-)} \\
&= N - \frac{4\kappa NK}{k_d(1+K)} \sum_{n=1}^{\infty} \frac{-\alpha_- e^{\alpha_+ t} (k_d + k_a + \alpha_+) + \alpha_+ e^{\alpha_- t} (k_d + k_a + \alpha_-)}{j_{0,n}^2 (\alpha_+ - \alpha_-)}. \tag{5.11b}
\end{aligned}$$

There are five parameters to be determined in this problem, and each can be determined using a best-fit curve to the intensity plot, which is sketched in Figure 1.4. N can be determined from the intensity plot at the end of the saturation phase ($t = 0^-$) as shown in (2.8a). κ can be determined at the beginning of the measurement phase ($t = 0^+$) as shown in (2.8b). (Note that this simplification is not immediately visible from (5.11b).)

To obtain a good starting guess for K , one can perform a logarithmic transformation of the data. As the system transitions from the diffusive to the kinetic regime, there should be a noticeable change in the trend line at the point labeled t_* (see Figure 1.4). The value of I there can be used to establish K . Since $r_\infty = \tilde{\omega}$ is known, D and k_a may be determined from the λ_n , which will fit the behavior of the curve in the evolution phase. Note that the most complicated part of the problem, the $j_{0,n}$, may be calculated once and stored in a table. Also note that k_d can be determined once K and k_a are known.

During the workshop, a Matlab implementation of (5.11b) was written. N and κ were estimated directly from the data, and the resulting values substituted into (5.11b). Then

this was fit (with 25 terms) against the data to determine D , K , and k_a . D was again always started with $D = 1 \mu\text{m}^2/\text{s}$. Four starting values of K and k_a were used, and the code runs 16 optimizations using all permutations of the sets.

First, we wish to try the kinetic model on data which has been determined to be diffusion-limited. We wish to check three key features of the new model:

1. The fit should not be worse (this is guaranteed by the fact that we have introduced another free parameter).
2. The previously determined values of D and K should not vary much from the values determined by the kinetics-free model.
3. The value of k_d determined should be low (pointing to small kinetics effects).

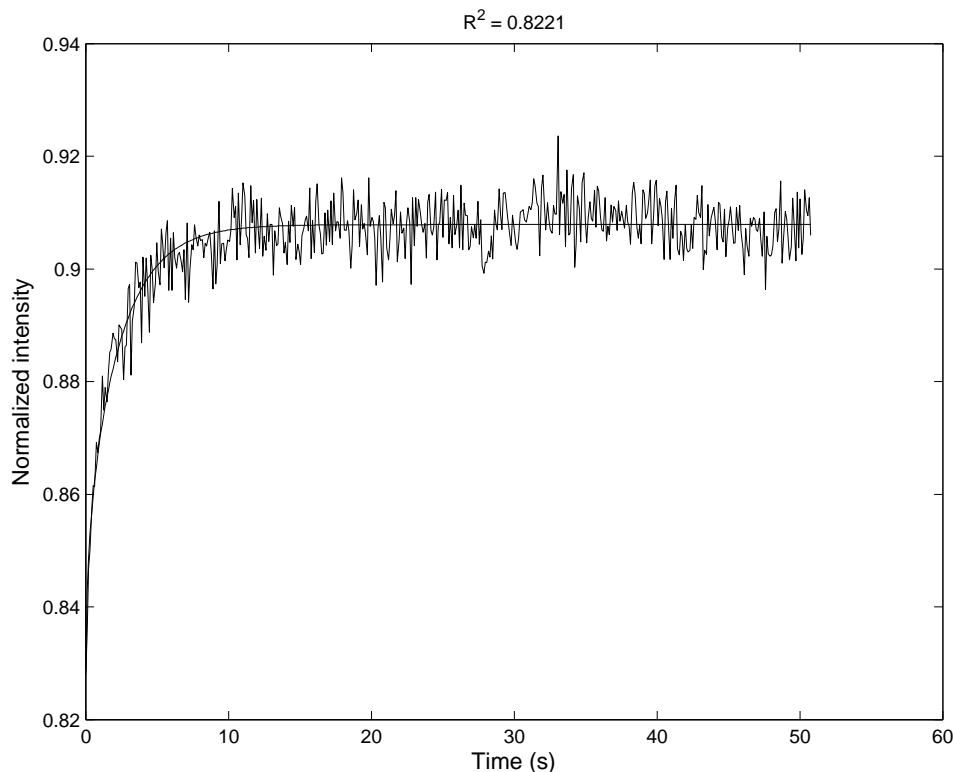


Figure 5.2. Data without obvious kinetic effects.

Figure 5.2 shows the same data as in figure 3.2, fit with both the kinetic and kinetics-free models. Note that the curve fits are nearly identical. The key parameters obtained are

$$D = 1.866 \frac{\mu\text{m}^2}{\text{s}}, \quad K = 18.27, \quad k_a = 7.47 \times 10^{-4} \text{ s}^{-1} \quad \implies \quad k_d = 1.36 \times 10^{-2} \text{ s}^{-1}. \quad (5.12)$$

Note the low value of k_d , indicating that kinetics are unimportant. Note also the close agreement between D in (3.21) and (5.12). However, there is a difference in K that must be explained. Also, note that the R^2 value for the plot increases only slightly, indicating that including the kinetics doesn't affect the plots very much.

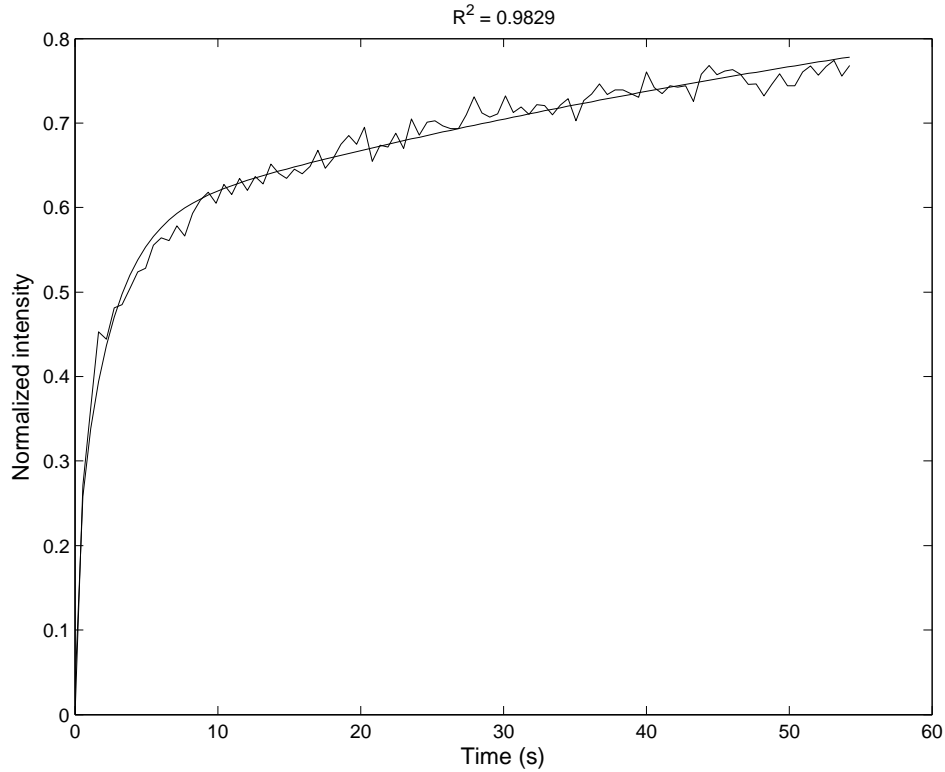


Figure 5.3. Data with kinetic effects.

Figure 5.3 shows the same data as in figure 3.3, fit with the kinetic model. Note that the curve fit with the kinetic model is much improved, since it captures the long-term linear uptick. The key parameters obtained are

$$D = 1.735 \frac{\mu\text{m}^2}{\text{s}}, \quad K = 1.403, \quad k_a = 8.547 \times 10^{-3} \text{ s}^{-1}, \quad \implies \quad k_d = 1.199 \times 10^{-2} \text{ s}^{-1}. \quad (5.13)$$

It is not entirely clear why the parameters behave in this manner, since one would expect k_d to be higher in this case. Also, the values of D and K are significantly different between (3.22) and (5.13) (but more trustworthy in the latter due to the improved fit, which can be seen from the increased R^2 values). Finally, note that the computed values of N and κ do not change, since they arise in preprocessing steps using the initial normalized intensity.

Section 6: Vertical Diffusion

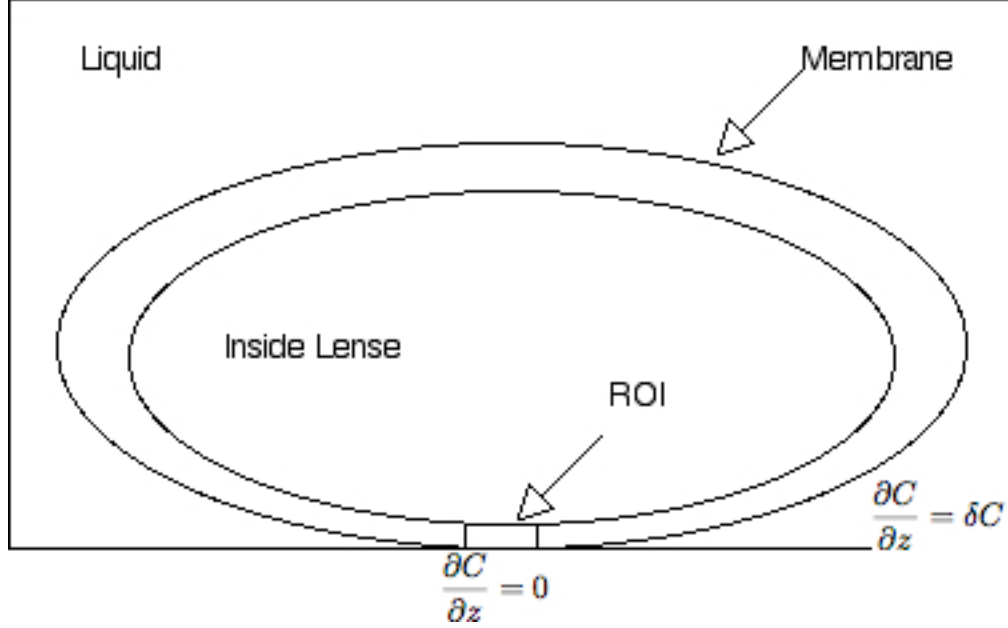


Figure 6.1. Schematics of experimental setup.

In actuality, the membrane is three-dimensional (see Figure 6.1). The lens rests on a microscope slide ($\tilde{z} = -h$), and hence there is no flux of molecules through this surface (see Figure 6.2). For large lenses, the weight of the lens is enough to squeeze the liquid from between the lens and the slide. For smaller lenses, additional weight should be added. The interior of the lens ($\tilde{z} = h$) is also impermeable to the molecules, so there is no flux there as well. These conditions motivate the scaling

$$\tilde{z} = hz. \quad (6.1)$$

The laser bleaches a cylindrically symmetric region $0 < r < \omega(z)$, which is also symmetric about the plane $\tilde{z} = 0$ (see Figure 6.2). Therefore we may solve the diffusion equation in the region $0 < z < 1$. Because of the curved nature of the bleaching zone, a one-compartment model is no longer useful. It would involve changing coordinates, which yielded complicated equations. Therefore, we proceed directly to the two-compartment model.

We begin by neglecting kinetics and solve the following diffusion equation:

$$\begin{aligned} \frac{\partial F^m}{\partial t} &= D \left[\frac{1}{\tilde{r}} \frac{\partial}{\partial \tilde{r}} \left(\tilde{r} \frac{\partial F^m}{\partial \tilde{r}} \right) + \frac{\partial^2 F^m}{\partial \tilde{z}^2} \right] \\ \frac{\partial F^m}{\partial t} &= D \left[\frac{1}{r_\infty^2 r} \frac{\partial}{\partial r} \left(r \frac{\partial F^m}{\partial r} \right) + \frac{1}{h^2} \frac{\partial^2 F^m}{\partial z^2} \right], \quad 0 < r < 1, \quad 0 < z < 1. \end{aligned} \quad (6.2)$$

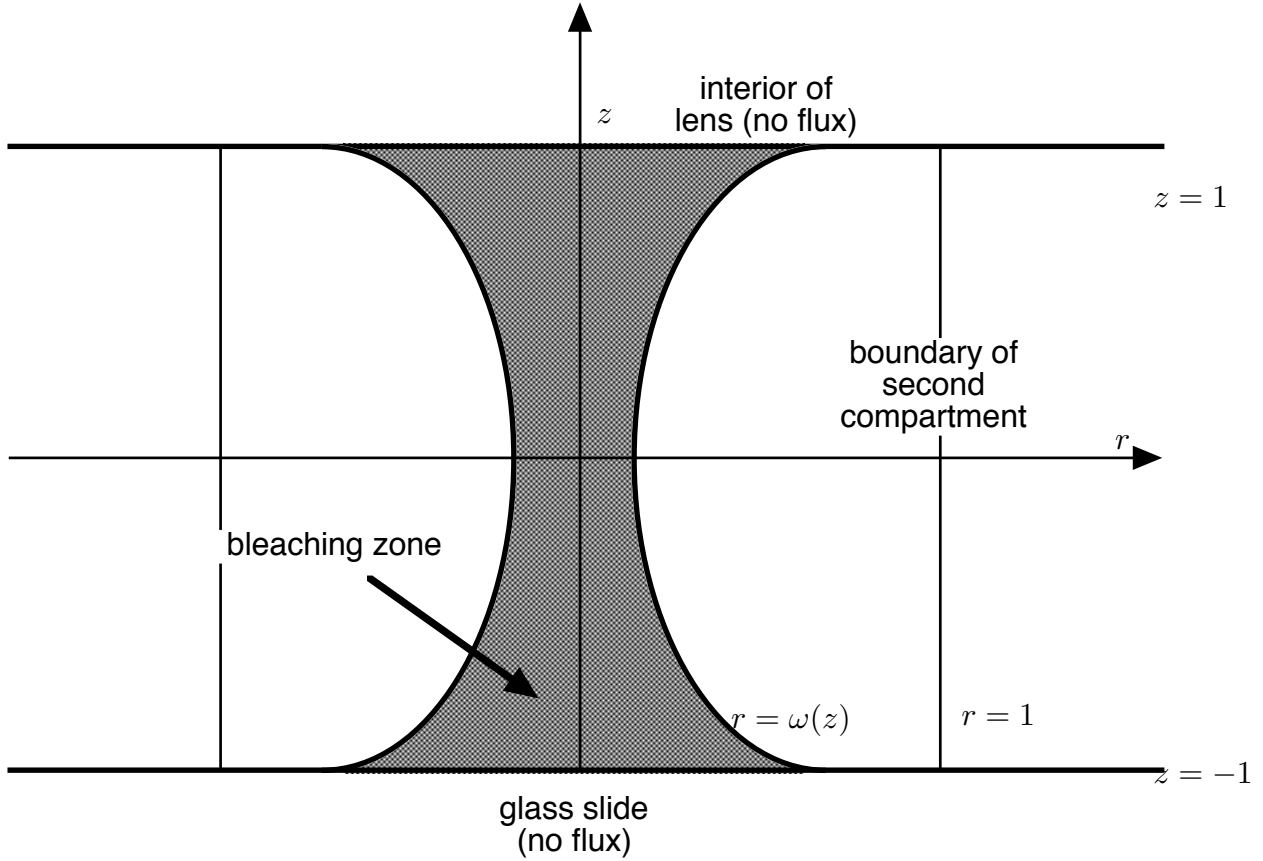


Figure 6.2. Plot of 3-D model.

Note that if $\omega(z)$ is a constant, F^m does not vary in the z -direction and we are reduced to the previous case.

To transform to homogeneous boundary conditions, we let

$$u^m(r, z, t) = F^m(r, z, t) - F_\infty^m \quad (6.3)$$

as before to obtain

$$u^m(1, z, t) = 0, \quad \frac{\partial u^m}{\partial z}(r, 0, t) = 0, \quad \frac{\partial u^m}{\partial z}(r, 1, t) = 0, \quad (6.4a)$$

$$u^m(r, z, 0) = -\kappa F_\infty^m [1 - H(r - \omega(z))]. \quad (6.4b)$$

where we have used our discussion about no flux through the boundaries, as well as the symmetry condition.

Separating variables by setting $u^m(r, t) = R(r)Z(z)T(t)$, we see that the r -dependence is exactly the same. So we have

$$\frac{T'}{T} = -\lambda_n + \frac{DZ''}{h^2 Z} = -\lambda_n - l_m$$

$$Z'' + \frac{l_m h^2}{D} Z = 0, \quad Z'(0) = Z'(1) = 0,$$

$$Z_m(z) = \cos m\pi z, \quad l_m = \frac{m^2\pi^2 D}{h^2}, \quad m = 0, 1, 2, \dots \quad (6.5a)$$

$$\lambda_{m,n}^* = \lambda_n + l_m = D \left(\frac{j_{0,n}^2}{r_\infty^2} + \frac{m^2\pi^2}{h^2} \right). \quad (6.5b)$$

$$T_{m,n}(t) = \exp(-\lambda_{m,n}^* t). \quad (6.6)$$

Then by the principle of superposition, we have the following:

$$u^m(r, t) = -F_\infty^m \sum_{m=0}^{\infty} \sum_{n=1}^{\infty} T_{m,n}(0) J_0(j_{0,n} r) \exp(-\lambda_{m,n}^* t) \cos(m\pi z), \quad (6.7)$$

where by the orthogonality properties of the Bessel and cosine functions we have that

$$\begin{aligned} T_{m,n}(0) &= \frac{2\kappa}{J_1^2(j_{0,n})} \left[\int_0^1 \cos(m\pi z) \int_0^1 r J_0(j_{0,n} r) \{[1 - H(r - \omega(z))]\} dr dz \right] \times \\ &\quad \left[\int_0^1 \cos^2(m\pi z) dz \right]^{-1} \\ &= \frac{4\kappa}{J_1^2(j_{0,n})(1 + \delta_{m0})} \int_0^1 \cos(m\pi z) \int_0^{\omega(z)} r J_0(j_{0,n} r) dr dz \\ &= \frac{4\kappa}{J_1^2(j_{0,n})j_{0,n}^2(1 + \delta_{m0})} \int_0^1 \cos(m\pi z) \int_0^{j_{0,n}\omega(z)} \rho J_0(\rho) d\rho dz \\ T_{m,n}(0) &= \frac{4\kappa\omega_{m,n}}{J_1^2(j_{0,n})j_{0,n}}, \end{aligned} \quad (6.8a)$$

$$\omega_{m,n} = \frac{1}{1 + \delta_{m0}} \int_0^1 \cos(m\pi z) \omega(z) J_1(j_{0,n}\omega(z)) dz, \quad (6.8b)$$

where δ is the Kronecker delta function, chosen to ensure the proper factor of 1/2 in front of the first Fourier coefficient.

We take the intensity measurement at $z = 0$, so we are interested in

$$F^m(r, 0, t) = F_\infty^m - F_\infty^m \sum_{m=0}^{\infty} \sum_{n=1}^{\infty} \frac{4\kappa\omega_{m,n}}{J_1^2(j_{0,n})j_{0,n}} J_0(j_{0,n} r) \exp(-\lambda_{m,n}^* t). \quad (6.9)$$

Since we are averaging only over the first compartment, the averaging proceeds as in (4.16) with $\omega = \omega(0)$. Thus we obtain (for the case of uniform sensing and bleaching)

$$\begin{aligned} I(t) &= \frac{(1 - \kappa)N}{1 + K} + \frac{KN}{1 + K} - \frac{NK}{1 + K} \sum_{m=0}^{\infty} \sum_{n=1}^{\infty} \frac{4\kappa\omega_{m,n}}{J_1^2(j_{0,n})j_{0,n}} \exp(-\lambda_{m,n}^* t) \left[\frac{2J_1(j_{0,n}\omega(0))}{\omega(0)j_{0,n}} \right] \\ &= \frac{(1 - \kappa + K)N}{1 + K} - \frac{8\kappa NK}{(1 + K)\omega(0)} \sum_{m=0}^{\infty} \sum_{n=1}^{\infty} \frac{\omega_{m,n} J_1(j_{0,n}\omega(0))}{J_1^2(j_{0,n})j_{0,n}^2} \exp(-\lambda_{m,n}^* t). \end{aligned} \quad (6.10)$$

Note that in the limit that $\omega(z)$ approaches a constant ω , the z -dependence drops out and so we are left with just one mode:

$$\begin{aligned}\lambda_{0,n}^* &= \lambda_n, \\ \omega_{0,n} &= \frac{1}{2} \int_0^1 \omega J_1(j_{0,n}\omega) dz = \frac{\omega J_1(j_{0,n}\omega)}{2}, \\ I(t) &= \frac{(1 - \kappa + K)N}{1 + K} - \frac{8\kappa NK}{(1 + K)\omega} \sum_{n=1}^{\infty} \frac{\omega_{0,n} J_1(j_{0,n}\omega)}{J_1^2(j_{0,n}) j_{0,n}^2} \exp(-\lambda_{0,n}^* t) \\ &= \frac{(1 - \kappa + K)N}{1 + K} - \frac{4\kappa NK}{1 + K} \sum_{n=1}^{\infty} \frac{J_1^2(j_{0,n}\omega)}{J_1^2(j_{0,n}) j_{0,n}^2} \exp(-\lambda_n t),\end{aligned}$$

which agrees with (4.16b).

Possibilities for Omega

Since (6.10) depends explicitly on the shape of the bleaching zone, we now discuss possible forms for $\omega(z)$. On physical grounds, we expect the surface to be a hyperboloid of one sheet, the equation of which would be given by

$$\begin{aligned}\omega^2(z) - b^2\omega^2(0)z^2 &= \omega^2(0) \\ \omega(z) &= \omega(0)\sqrt{1 + b^2z^2},\end{aligned}\tag{6.11}$$

where b is a fitting constant. For a simpler model, one could simply take a parabola:

$$\omega(z) = \omega(0)(1 + b^2z^2),\tag{6.12}$$

where we have kept in mind that $\omega(z)$ must be even in z . Note that (6.11) can be reduced to (6.12) (with suitable rescaling) for small b .

Measurements have shown that the value of b differs between mouse lenses and human lenses. It is not clear as to whether this is due to experimental error, or differences in makeup of the matrix. If the experimentalists are confident that both lenses should be modeled by the same curve, then another parameter would have to be introduced through a more complicated curve, for example:

$$\omega(z) = \omega(0)(1 + b_1^2z^2 + b_2^2z^4).$$

Section 7: Including Measurement Bleaching

Note from Figure 1.5 that both the control and bleached regions have an underlying decay to them. This is because even though the laser is operated at low power during the measurement phase, that low power still continually bleaches molecules. If one assumes that this forces a simple exponential decay onto the control data:

$$I_{\text{control}}(t) = I_{\text{control}}(0) \exp(-k_{\text{b}}t), \quad (7.1)$$

where the subscript “b” stands for “bleaching”, then one could divide by $I_{\text{control}}(t)$ to get a “normalized” $I(t)$ that would be free of the $\exp(-k_{\text{b}}t)$ dependence, and hence the measurement bleaching. These are the plots that were fit in previous sections.

Unfortunately, the same diffusion of unbleached molecules will also occur in the control region, so the mathematical situation is more complicated than that postulated in (7.1). In this section (completed after the close of the workshop, when this mechanism was more fully understood), we present more refined models of the system.

The measurement process will affect the immobile and mobile fractions in a manner proportional to their number. Therefore, in the kinetics-free case using the one-compartment model of section 3, we have

$$\frac{\partial F^{\text{m}}}{\partial t} = \frac{D}{r_{\infty}^2 r} \frac{\partial}{\partial r} \left(r \frac{\partial F^{\text{m}}}{\partial r} \right) - k_{\text{b}} F^{\text{m}}, \quad 0 < r < 1, \quad (7.2a)$$

$$\frac{\partial F^{\text{i}}}{\partial t} = -k_{\text{b}} F^{\text{i}}, \quad 0 < r < 1. \quad (7.2b)$$

Solving (7.2b) subject to (2.5a), we immediately obtain

$$F^{\text{i}}(t) = F_0^{\text{i}} \exp(-k_{\text{b}}t). \quad (7.3)$$

There are several ways to solve (7.2a). One achieves fast convergence of the sum, while the other can be computed quickly (and is hence preferred).

Fast Convergence Method

In order to achieve the fastest convergence of the sum, we subtract off the steady state of (7.2a) subject to (3.5b). In order to simplify later algebra, we let

$$F_{\text{steady}}^{\text{m}}(r) = F_{\infty}^{\text{m}} G(r),$$

in which case we obtain

$$\begin{aligned} \frac{D(rG')'}{r_{\infty}^2 r} - k_{\text{b}} G &= 0 \\ rG'' + G' - \frac{k_{\text{b}} r_{\infty}^2}{D} rG &= 0, \quad G(1) = 1. \end{aligned} \quad (7.4)$$

Equation (7.4) is in exactly the same form as (3.10) except for the sign of the second term, which makes it a modified Bessel equation. Therefore, we have that

$$G(r) = \frac{I_0(\delta r)}{I_0(\delta)}, \quad \delta = r_\infty \sqrt{\frac{k_b}{D}} \quad (7.5)$$

Note that as $k_b \rightarrow 0$, $\delta \rightarrow 0$ and $F_\infty^m G(r) \rightarrow F_\infty^m$, so we reduce to the previous case.

Then letting

$$\frac{F_\infty^m(r, t)}{F_\infty^m} - G(r) = \exp(-k_b t) u^m(r, t) \quad (7.6)$$

into (7.2a), (2.5b), and (3.5b), we obtain

$$\begin{aligned} \frac{\partial}{\partial t} (F_\infty^m [\exp(-k_b t) u^m + G]) &= \frac{D}{r_\infty^2 r} \frac{\partial}{\partial r} \left(r \frac{\partial}{\partial r} (F_\infty^m [\exp(-k_b t) u^m + G]) \right) \\ &\quad - k_b (F_\infty^m [\exp(-k_b t) u^m + G]) \\ \exp(-k_b t) \left(\frac{\partial u^m}{\partial t} - k_b u^m \right) &= \exp(-k_b t) \frac{D}{r_\infty^2 r} \frac{\partial}{\partial r} \left(r \frac{\partial u^m}{\partial r} \right) - k_b \exp(-k_b t) u^m \\ &\quad + \frac{D(rG)'}{r_\infty^2 r} - k_b G \\ \frac{\partial u^m}{\partial t} &= \frac{D}{r_\infty^2 r} \frac{\partial}{\partial r} \left(r \frac{\partial u^m}{\partial r} \right), \end{aligned} \quad (7.7)$$

$$u^m(r, 0) = \frac{F_0^m}{F_\infty^m} - G(r) = 1 - \kappa - G(r) = -(\kappa - 1 + G(r)), \quad (7.8a)$$

$$u^m(1, t) = 0. \quad (7.8b)$$

But (7.7) and (7.8) are in exactly the same form as (3.9) as modified in section 4 under the ‘‘nonuniform bleaching’’ assumption, with

$$\kappa(r) = \kappa - 1 + G(r). \quad (7.9)$$

Note that as $\delta \rightarrow 0$, $G(r) \rightarrow 1$ and $\kappa(r) \rightarrow \kappa$, reducing to the previous case. Therefore, we have the following:

$$u^m(r, t) = - \sum_{n=1}^{\infty} \frac{2[a_n(\kappa)]}{J_1^2(j_{0,n})} J_0(j_{0,n} r) \exp(-\lambda_n t), \quad (7.10a)$$

$$F_\infty^m(r, t) = F_\infty^m G(r) - \exp(-k_b t) F_\infty^m \sum_{n=1}^{\infty} \frac{2[a_n(\kappa)]}{J_1^2(j_{0,n})} J_0(j_{0,n} r) \exp(-\lambda_n t). \quad (7.10b)$$

$$I(t) = \frac{(1 - \kappa)N}{1 + K} \exp(-k_b t) + \frac{NK}{1 + K} \left[2 \int_0^1 r \frac{I_0(\delta r)}{I_0(\delta)} dr \right]$$

$$\begin{aligned}
& -\frac{NK}{1+K} \sum_{n=1}^{\infty} \frac{2[a_n(\kappa)][2a_n(1)]}{J_1^2(j_{0,n})} \exp(-(k_b + \lambda_n)t) \\
& = \frac{(1-\kappa)N}{1+K} \exp(-k_b t) + \frac{NK}{1+K} \left[\frac{2}{\delta^2 I_0(\delta)} \int_0^\delta \rho I_0(\rho) d\rho \right] \\
& \quad - \frac{4NK}{1+K} \sum_{n=1}^{\infty} \frac{a_n(\kappa) \exp(-(k_b + \lambda_n)t)}{j_{0,n} J_1(j_{0,n})} \\
& = \frac{(1-\kappa)N}{1+K} \exp(-k_b t) + \frac{NK}{1+K} \frac{2I_1(\delta)}{\delta I_0(\delta)} - \frac{4NK}{1+K} \sum_{n=1}^{\infty} \frac{a_n(\kappa) \exp(-(k_b + \lambda_n)t)}{j_{0,n} J_1(j_{0,n})},
\end{aligned} \tag{7.11}$$

where the integral is given by Bell, Theorem 4.15(i). Note that it is clear that as $t \rightarrow \infty$, the solution reduces to the steady state. Also, note that as $\delta \rightarrow 0$, $I_1(\delta) \rightarrow \delta/2$ and we are reduced to the previous case.

The main problem with (7.11) is that one of the fitting parameters, k_b , is buried inside the integral in $a_n(\kappa)$. This will make the optimization much more time consuming. One could think of estimating k_b from the control data. But the control data has the same problem with unbleached molecules diffusing in from outside. If the diffusion is slow enough, you might be able to get away with making a rough fit for k_b from the data. This would essentially make the control intensity a single exponential, justifying (7.1) and hence the data previously fit.

Speedy Computation Method

Since the previous method seems unsuitable for curve fitting, we take the simpler approach of simply substituting (3.8) into (7.2), which yields

$$\frac{\partial u^m}{\partial t} = \frac{D}{r_\infty^2 r} \frac{\partial}{\partial r} \left(r \frac{\partial u^m}{\partial r} \right) - k_b (u^m + F_\infty^m), \tag{7.12}$$

subject to (3.9b). This operator is somewhat similar to that in (4.4a), so we use the series solution in (4.5) to obtain (for the case of uniform bleaching)

$$\begin{aligned}
\frac{dT_n^m}{dt} & = -\lambda_n T_n^m - k_b T_n^m - k_b F_\infty^m a_n(1), \quad T_n^m(0) = -\kappa F_\infty^m a_n(1), \\
T_n^m & = -F_\infty^m a_n(1) \left[\frac{k_b}{\lambda_n + k_b} + \left(\kappa - \frac{k_b}{\lambda_n + k_b} \right) \exp(-(\lambda_n + k_b)t) \right], \\
u^m(r, t) & = -2F_\infty^m \sum_{n=1}^{\infty} \frac{J_0(j_{0,n}r)}{J_1(j_{0,n})j_{0,n}} \left[\frac{k_b}{\lambda_n + k_b} + \left(\kappa - \frac{k_b}{\lambda_n + k_b} \right) \exp(-(\lambda_n + k_b)t) \right], \\
F^m(r, t) & = F_\infty^m - 2F_\infty^m \sum_{n=1}^{\infty} \frac{J_0(j_{0,n}r)}{J_1(j_{0,n})j_{0,n}} \left[\frac{k_b}{\lambda_n + k_b} + \left(\kappa - \frac{k_b}{\lambda_n + k_b} \right) \exp(-(\lambda_n + k_b)t) \right],
\end{aligned}$$

(7.13a)

$$I(t) = \frac{(1 - \kappa)N}{1 + K} \exp(-k_b t) + \frac{NK}{1 + K} - \frac{4NK}{1 + K} \sum_{n=1}^{\infty} \frac{1}{j_{0,n}^2} \left[\frac{k_b}{\lambda_n + k_b} + \left(\kappa - \frac{k_b}{\lambda_n + k_b} \right) \exp(-(\lambda_n + k_b)t) \right], \quad (7.13b)$$

where we have used the fact that this is mostly a repetition of previously-done work. Note that in the limit that $k_b \rightarrow 0$, (7.13b) reduces to (3.20).

Though the convergence of this sum may be somewhat slower, it avoids the problem of having to fit k_b inside any sort of integral term.

Including Kinetics

Motivated by the previous section, we now use the same trick to include kinetic effects. In this case, (5.1) becomes

$$\frac{\partial F^m}{\partial t} = \frac{D}{r_\infty^2 r} \frac{\partial}{\partial r} \left(r \frac{\partial F^m}{\partial r} \right) - k_a F^m + k_d F^i - k_b F^m, \quad (7.14a)$$

$$\frac{\partial F^i}{\partial t} = k_a F^m - k_d F^i - k_b F^i, \quad (7.14b)$$

which, upon substituting (5.2), become

$$\frac{\partial u^m}{\partial t} = \frac{D}{r_\infty^2 r} \frac{\partial}{\partial r} \left(r \frac{\partial u^m}{\partial r} \right) - (k_a + k_b) u^m + k_d u^i - k_b F_\infty^m, \quad (7.15a)$$

$$\frac{\partial u^i}{\partial t} = -(k_d + k_b) u^i + k_a u^m - k_b F_\infty^i. \quad (7.15b)$$

The boundary and initial data are given by (5.4) and (3.9b).

Motivated by (4.5), we adapt (5.7) by removing the $-\kappa$ term, since by (7.13a) we see that it isn't going to appear as a coefficient:

$$u^i(r, t) = \sum_{n=1}^{\infty} \frac{2T_n^i(t)}{J_1(j_{0,n})} \frac{J_0(j_{0,n}r)}{j_{0,n}}, \quad T_n^i(t) = \frac{1}{a_n(1)} \int_0^1 r u^i(r, t) J_0(j_{0,n}r) dr, \quad (7.16a)$$

$$u^m(r, t) = \sum_{n=1}^{\infty} \frac{2T_n^m(t)}{J_1(j_{0,n})} \frac{J_0(j_{0,n}r)}{j_{0,n}}, \quad T_n^m(t) = \frac{1}{a_n(1)} \int_0^1 r u^m(r, t) J_0(j_{0,n}r) dr. \quad (7.16b)$$

In this case, our initial conditions are given by

$$T_n^i(0) = -\kappa F_\infty^i, \quad T_n^m(0) = -\kappa F_\infty^m. \quad (7.17)$$

Substituting (7.16) into (7.15), we see that the equations analogous to (5.8a) become

$$\frac{d}{dt} \begin{pmatrix} T_n^m \\ T_n^i \end{pmatrix} = A \begin{pmatrix} T_n^m \\ T_n^i \end{pmatrix} - k_b \begin{pmatrix} F_\infty^m \\ F_\infty^i \end{pmatrix}, \quad A = \begin{pmatrix} -\lambda_n - k_a - k_b & k_d \\ k_a & -k_d - k_b \end{pmatrix}.$$

Note that by maintaining a positive sign on our series in (7.16), we don't have to worry about changing the signs of the forcing terms. Solving the above, we have

$$\begin{pmatrix} T_n^m \\ T_n^i \end{pmatrix} = k_b A^{-1} \begin{pmatrix} F_\infty^m \\ F_\infty^i \end{pmatrix} + c_+ e^{(\alpha_+ - k_b)t} \mathbf{v}_+ + c_- e^{(\alpha_- - k_b)t} \mathbf{v}_-, \quad (7.18a)$$

$$A^{-1} = \frac{1}{(\alpha_+ - k_b)(\alpha_- - k_b)} \begin{pmatrix} -k_d - k_b & -k_d \\ -k_a & -\lambda_n - k_a - k_b \end{pmatrix}. \quad (7.18b)$$

where we have used linear algebra properties to relate the eigenvalues and eigenvectors of our new A to the A in section 5.

From (7.17) we see that initial conditions for the problem are given by

$$\begin{pmatrix} T_n^m \\ T_n^i \end{pmatrix} (0) = k_b A^{-1} \begin{pmatrix} F_\infty^m \\ F_\infty^i \end{pmatrix} + c_+ \mathbf{v}_+ + c_- \mathbf{v}_- = - \begin{pmatrix} \kappa F_\infty^m \\ \kappa F_\infty^i \end{pmatrix}.$$

Solving the above for the c_\pm , we obtain

$$\begin{aligned} V \begin{pmatrix} c_+ \\ c_- \end{pmatrix} &= -(\kappa I + k_b A^{-1}) \begin{pmatrix} F_\infty^m \\ F_\infty^i \end{pmatrix}, \quad V = \begin{pmatrix} k_d + \alpha_+ & k_d + \alpha_- \\ k_a & k_a \end{pmatrix} \\ \begin{pmatrix} c_+ \\ c_- \end{pmatrix} &= -V^{-1}(\kappa I + k_b A^{-1}) \begin{pmatrix} F_\infty^m \\ F_\infty^i \end{pmatrix}. \end{aligned} \quad (7.19)$$

We could write down the complicated expressions, but as the inversion can be done more conveniently in Matlab, we leave the solution in this form.

For the intensity, we are interested in

$$\begin{aligned} T_n^i(t) + T_n^m(t) &= k_b \frac{(-k_d - k_b - k_a)F_\infty^m + (-\lambda_n - k_a - k_b - k_d)F_\infty^i}{(\alpha_+ - k_b)(\alpha_- - k_b)} \\ &\quad + c_+ e^{(\alpha_+ - k_b)t} (k_d + k_a + \alpha_+) + c_- e^{(\alpha_- - k_b)t} (k_d + k_a + \alpha_-) \\ &= -k_b \frac{(k_d + k_b + k_a)(F_\infty^m + F_\infty^i) + \lambda_n F_\infty^i}{(\alpha_+ - k_b)(\alpha_- - k_b)} + c_+ e^{(\alpha_+ - k_b)t} (k_d + k_a + \alpha_+) \\ &\quad + c_- e^{(\alpha_- - k_b)t} (k_d + k_a + \alpha_-) \\ &= -k_b \frac{(k_d + k_b + k_a)N + \lambda_n F_\infty^i}{(\alpha_+ - k_b)(\alpha_- - k_b)} + c_+ e^{(\alpha_+ - k_b)t} (k_d + k_a + \alpha_+) \\ &\quad + c_- e^{(\alpha_- - k_b)t} (k_d + k_a + \alpha_-). \end{aligned} \quad (7.20)$$

where we have used (3.2).

Therefore, our expression in (5.11a) is replaced by

$$I(t) = N + 4 \sum_{n=1}^{\infty} \frac{T_n^i(t) + T_n^m(t)}{j_{0,n}^2}, \quad (7.21)$$

where the summand is defined as in (7.20).

Section 8: Conclusions and Further Research

The purpose of this work was to study diffusion through the lens capsule, in particular to estimate diffusion rates of various molecules through the capsule from data resulting from fluorescence recover after photobleaching (FRAP) experiments.

Previously, the post-experiment data processing was done by fitting a linear combination of one or two exponentials with 3 or 5 independent parameters to the normalized data (which accounts for the fact that fluorescence decreases with time). This was clearly just an *ansatz* based on the expected exponential decay of intensity with time which failed to account for the nature of diffusion, namely that different time scales for decay are all related (eigenvalues of a Sturm-Liouville problem), as well as the amplitudes of the different modes.

Experimentalists observed strong sensitivity of the parameter estimation to the time used to truncate the data — an obviously unsettling fact that leads to lack of confidence in the method they were using. A better analysis was needed to derive a more robust technique for parameter estimation.

Various mathematical models were derived accounting for different processes, geometries and inhomogeneities. All models assume bleaching in a radially symmetric region to be radially symmetric, which seems to agree fairly well with experimental observation. During the measurement phase of the experiments (starting just after bleaching) fluorescing particles are either bound (immobile) or free to diffuse (mobile), and uniformly distributed throughout the membrane, with a constant total concentration due to transport equilibrium. The concentration of bound and mobile particles can change due to association and dissociation reactions, which are assumed to follow simple mass-action kinetics. It's also assumed that the particles are in chemical equilibrium just before bleaching, with the relative concentrations of mobile and immobile particles depending on an *affinity constant*; no shortage of binding sites is also assumed.

The following cases were considered. In all cases Dirichlet data is given on a circle large enough across which the lens will transport any needed particles very quickly.

1. Diffusion much faster than reaction, in which case a one-compartment, no kinetics model was derived (Section 3). A Matlab code was written to implement the Bessel-Fourier series solution and to find a best fit for the parameters to the data. For “large” molecules the fit was very good, but for smaller molecules kinetics is expected to play a role, and it should be incorporated in the model.
2. In Section 4, extensions were considered. First, the case of non-uniform bleaching (bleaching fraction is a function of radial position) was analyzed, and the appropriate modification derived, but not implemented in Matlab. Second, non-uniform sensing was included and the series solution for the intensity derived. Finally, we considered a two-compartment model with the (uniform) bleaching zone embedded in a larger diffusion region. This introduces another parameter ω , the ratio of the radius of the bleaching zone to that of the diffusion region, which has to be estimated as well.

3. The one-compartment model including kinetics is derived in Section 5. This introduces another parameter (a rate of reaction constant) to be estimated. A formula (infinite series) for the intensity was derived and used in a Matlab code to estimate the parameters. As expected, a check of the fit with both kinetics and kinetics-free models, for the case of data showing a diffusion dominated process, resulted in nearly identical fit, with the extra parameter (the reaction rate) being very small, but with some variation in the affinity constant which is not explained. The fit for the case of smaller molecules (which was not good for the kinetics-free model) is much better with kinetics included. The diffusion coefficient and the affinity coefficients changed significantly from those fit with the kinetics-free model. One can conjecture that smaller molecules are more likely to undergo association, thus corresponding to different values of the affinity parameter as compared to the larger molecules; this is the trend observed with the two sets of data. Also, the kinetics model includes the details of reactions that may have a cumulative effect on the solution over time, thus affecting the parameters that produce the best fit, perhaps explaining the variations observed in the diffusion and affinity coefficients with the small molecule data.
4. In Section 6 a model that includes diffusion in the axial direction is derived to account for a possible radially symmetric axial variation of the radius of the bleaching zone. The formula for the intensity (infinite series) is derived — it depends on the particular shape of the bleaching zone.
5. Finally, in Section 7, a more refined model accounts for the continuation of bleaching during the measurement phase (the laser is still on, although operated at a much lower power). The one-compartment models of Sections 3 and 5 are refined to include the bleaching kinetics during the measurement phase. These have also been implemented in Matlab code.

In the future, the solution of a two-compartment reaction-diffusion model, including the kinetics of bleaching in the measurement phase, can be attempted to determine if more consistency is achieved on large molecule particles for models with and without kinetics. Additionally, axial diffusion can be added to obtain a more complete model. Matlab implementation should be done with all reasonable models for comparison, so that a conclusion may be reached as to which model is sufficiently robust to be routinely used for work with the lens capsule.

Nomenclature

If the same letter appears both with and without tildes, the variable with a tilde has dimensions, while the one without is dimensionless. The equation number where a particular quantity first appears is listed, if appropriate.

- A : matrix arising in kinetics solution (5.8a).
- $a_n(\cdot)$: constant arising in separation-of-variables solution (3.15).
- $B(\tilde{r}, t)$: concentration of bleached particles at position (\tilde{r}, t) (2.6).
 - b : fitting constant for $\omega(z)$ (6.11).
 - c : constant in kinetics solution (5.8b).
- D : diffusion coefficient.
- $F(\tilde{r}, \tilde{z}, \theta, t)$: concentration of fluorescent particles at position $(\tilde{r}, \tilde{z}, \theta, t)$ (2.1).
 - $f(\cdot)$: arbitrary function.
 - h : half-height of membrane (6.1).
- $I(t)$: averaged intensity at time t (1.1).
 - K : affinity constant, defined as k_d/k_a (2.3b).
 - k : rate constant (2.2).
- l_m : eigenvalue related to the eigenfunction of the diffusion operator in the z -direction (6.5a).
- m : indexing variable.
- N : total concentration of particles (2.1).
- n : indexing variable.
- $R(r)$: component of separation-of-variables solution (3.10).
 - \tilde{r} : radial coordinate (2.1).
- $S(r)$: strength of intensity measurement (4.10).
- $T(t)$: component of separation-of-variables solution (3.12).
 - t : time coordinate (1.1).
- $u(r, z, t)$: component of separation-of-variables solution (3.8).
 - \mathbf{v} : eigenvector of A (5.8b).
 - \mathcal{Z} : the integers.
- $Z(z)$: component of separation-of-variables solution (6.5a).
 - \tilde{z} : height above measurement plane (6.1).
 - α : eigenvalue of A (5.8b).
- γ_D : correction coefficient in estimating D from $\tau_{1/2}$.
- δ : parameter in steady-state solution (7.5).
- θ : angular coordinate (2.7).
- $\kappa(r)$: bleaching fraction.
 - λ : eigenvalue related to the eigenfunction of the diffusion operator.
 - ρ : dummy variable of integration.
 - τ : time constant, variously defined.

$\tilde{\omega}(\tilde{z})$: radius of region of interest.

Other Notation

- a: as a subscript, used to indicate association (2.2).
- b: as a subscript, used to indicate bleaching (7.1).
- d: as a subscript, used to indicate dissociation (2.2).
- i: as a superscript, used to indicate immobile (2.1).
- m: as a superscript, used to indicate mobile (2.1).
- $n \in \mathcal{Z}$: as a sub- or superscript, used to indicate a mode in an eigenfunction expansion (3.11a) or simple indexing (1.1).
- 0: as a subscript on F , used to indicate an initial condition (2.5).
- 1/2: as a subscript on τ , used to indicate a time constant (1.1).
- ∞ : as a subscript, used to indicate an exterior value (3.2).

References

- Axelrod, D., Koppel, D. E., Schlessinger, J., Elson, E., Webb, W.W. “Mobility Measurement by Analysis of Fluorescence Photobleaching Recovery Techniques.” *Biophysical J.*, **16**, pp. 1055-1069 (1976).
- Bell, W. W. *Special Functions for Scientists and Engineers*. London: D. van Nostrand, 1968.
- Carslaw, H. S., and Jaeger, J. C. *Conduction of Heat in Solids*, 2nd ed. London: Oxford, 1959.
- Sprague, B. L., Pego, R. L, Stavreva, D. A., and McNally, J. G. “Analysis of Binding Reactions by Fluorescence Recovery after Photobleaching.” *Biophysical J.*, **86**, pp. 3473–3495 (2004).